

AD-A251 241



2

PL-TR-92-2019

PERSISTENCE OF AURORAL ELECTRON FLUX EVENTS
FROM DMSP/F9 ELECTRON MEASUREMENTS

K. H. Bounar
W. J. McNeil

Radex, Inc.
Three Preston Court
Bedford, MA 01730



January 31, 1992

Scientific Report No. 3

Approved for public release; distribution unlimited




PHILLIPS LABORATORY
AIR FORCE SYSTEMS COMMAND
HANSCom AIR FORCE BASE, MASSACHUSETTS 01731-5000

92-13348



92 5 10 018

"This technical report has been reviewed and is approved for publication"



ROBERT J. RAISTRICK
Contract Manager
Data Analysis Division



ROBERT E. MCINERNEY, Director
Data Analysis Division

This report has been reviewed by the ESD Public Affairs Office (PA) and is releasable to the National Technical Information Service (NTIS).

Qualified requestors may obtain additional copies from the Defense Technical Information Center. All others should apply to the National Technical Information Service.

If your address has changed, or if you wish to be removed from the mailing list, or if the addressee is no longer employed by your organization, please notify GL/IMA, Hanscom AFB, MA 01731. This will assist us in maintaining a current mailing list.

Do not return copies of this report unless contractual obligations or notices on a specific document requires that it be returned.

REPORT DOCUMENTATION PAGE			Form Approved OMB No. 0704-0188	
<small>Public reporting burden for this collection of information is estimated to average 1 hour per response, including the time for reviewing instructions, searching existing data sources, gathering and maintaining the data needed, and completing and reviewing the collection of information. Send comments regarding this burden estimate or any other aspect of this collection of information, including suggestions for reducing this burden, to Washington Headquarters Services, Directorate for Information Operations and Reports, 1215 Jefferson Davis Highway, Suite 1204, Arlington, VA 22202-4302, and to the Office of Management and Budget, Paperwork Reduction Project (0704-0188), Washington, DC 20503.</small>				
1. AGENCY USE ONLY (Leave blank)	2. REPORT DATE 31 January 1992	3. REPORT TYPE AND DATES COVERED Scientific Report No. 3		
4. TITLE AND SUBTITLE Persistence of Auroral Electron Flux Events From DMSP/F9 Electron Measurements		5. FUNDING NUMBERS PE 62101F PR S321 TA 85 WU AC Contract F19628-90-C-0191		
6. AUTHOR(S) K. H. Bounar W. J. McNeil				
7. PERFORMING ORGANIZATION NAME(S) AND ADDRESS(ES) RADEX, Inc. Three Preston Court Bedford, MA 01730		8. PERFORMING ORGANIZATION REPORT NUMBER RXR-92012		
9. SPONSORING/MONITORING AGENCY NAME(S) AND ADDRESS(ES) Phillips Laboratory Hanscom AFB, MA 01731-5000 Contract Manager: Robert J. Raistrick/GPD		10. SPONSORING/MONITORING AGENCY REPORT NUMBER PL-TR-92-2019		
11. SUPPLEMENTARY NOTES				
12a. DISTRIBUTION/AVAILABILITY STATEMENT Approved for Public Release Distribution Unlimited		12b. DISTRIBUTION CODE		
13. ABSTRACT (Maximum 200 words) The persistence of auroral electron activity is examined and correlated to the geomagnetic activity, which is measured by the Kp index. To study this correlation the superposed epoch analysis technique was implemented. Epoch zero is the time at which Kp values persisted above a specified threshold value for a specified duration. It was found that a high correlation between enhanced Kp and the number of bright arcs can be achieved for a limited time. The waiting time to increase the chance of observing bright auroral arcs after enhanced Kp values are observed should be between 3 to 6 hours. Further, the substantial increase in the number of observations of intense events as a result of enhanced Kp lingers a maximum of 36 to 48 hours. After this time period, this number drops to the average number of random observations.				
14. SUBJECT TERMS Defense Meteorological Satellite Program (DMSP), Aurora, Precipitating electrons, Geomagnetic Kp index, Superposed epoch analysis			15. NUMBER OF PAGES 54	
			16. PRICE CODE	
17. SECURITY CLASSIFICATION OF REPORT Unclassified	18. SECURITY CLASSIFICATION OF THIS PAGE Unclassified	19. SECURITY CLASSIFICATION OF ABSTRACT Unclassified	20. LIMITATION OF ABSTRACT Unlimited	

TABLE OF CONTENTS

<u>Section</u>	<u>Page</u>
1.0 INTRODUCTION	1
2.0 DATA BASE GENERATION	1
3.0 APPROACH	3
4.0 DISCUSSION OF THE RESULTS	4
4.1 K _p CHARACTERISTICS	5
4.2 ELECTRON EVENTS CHARACTERISTICS	5
4.3 COMPARISON OF K _p AND ELECTRON EVENTS	14
5.0 CONCLUSION AND FUTURE STUDIES	31
6.0 REFERENCES	32
APPENDIX A. GEOMAGNETIC K _p INDEX AND AURORAL EVENTS	33



Accession For	
NTIS GRA&I	<input checked="" type="checkbox"/>
DTIC TAB	<input type="checkbox"/>
Unannounced	<input type="checkbox"/>
Justification	
By	
Distribution/	
Availability Codes	
Dist	Avail and/or Special
A-1	

LIST OF FIGURES

<u>Figure</u>	<u>Page</u>
1. Kp index and number of auroral events with energy fluxes greater or equal to 2 kR observed in each hemispheric pass. These data are based on DMSP/F9 flux measurements in 1990.	2
2(a). Superposed epochs of Kp index over a time window of 4 days with a sampling rate of 1.2 hours. Seven curves are plotted, each corresponding to a different Kp threshold. This figure is for a Kp persistence time of 3 hours.	6
2(b). Same as Figure 2(a), but for a Kp persistence time of 6 hours.	7
2(c). Same as Figure 2(a), but for a Kp persistence time of 9 hours.	8
2(d). Same as Figure 2(a), but for a Kp persistence time of 12 hours.	9
3(a). Superposed epochs of the number of events per hemispheric pass for energy fluxes (JEtot) greater than or equal to 2 kR over a time window of 4 days with a sampling rate of 1.2 hours. Seven curves are plotted, each corresponding to a different Kp threshold (same as Figure 2). This figure is for a Kp persistence time of 3 hours.	10
3(b). Same as Figure 3(a), but for a Kp persistence time of 6 hours.	11
3(c). Same as Figure 3(a), but for a Kp persistence time of 9 hours.	12
3(d). Same as Figure 3(a), but for a Kp persistence time of 12 hours.	13
4(a). Same as Figure 3(a), except that $J_{Etot} \geq 6$ kR.	15
4(b). Same as Figure 3(b), except that $J_{Etot} \geq 6$ kR.	16
4(c). Same as Figure 3(c), except that $J_{Etot} \geq 6$ kR.	17
4(d). Same as Figure 3(d), except that $J_{Etot} \geq 6$ kR.	18

List of Figures (cont'd)

<u>Figure</u>	<u>Page</u>
5(a). Same as Figure 3(a), except that $JE_{tot} \geq 20$ kR.	19
5(b). Same as Figure 3(b), except that $JE_{tot} \geq 20$ kR.	20
5(c). Same as Figure 3(c), except that $JE_{tot} \geq 20$ kR.	21
5(d). Same as Figure 3(d), except that $JE_{tot} \geq 20$ kR.	22
6(a). Same as Figure 3(a), except that $JE_{tot} \geq 60$ kR.	23
6(b). Same as Figure 3(b), except that $JE_{tot} \geq 60$ kR.	24
6(c). Same as Figure 3(c), except that $JE_{tot} \geq 60$ kR.	25
6(d). Same as Figure 3(d), except that $JE_{tot} \geq 60$ kR.	26
7(a). Comparison of Kp index with the number of events per hemispheric pass for energy fluxes (JE_{tot}) greater than or equal to 2 kR over a time window of 4 days with a sampling rate of 1.2 hours. The solid line is the smoothed number of events which are the 3-point averages of the samples denoted by plus signs (+). The dashed line is the 3-point smoothed Kp. This figure is for a Kp threshold of 4.0 and a Kp persistence time of 3 hours.	27
7(b). Same as Figure 7(a), but for an energy flux threshold of 6 kR.	28
7(c). Same as Figure 7(a), but for an energy flux threshold of 20 kR.	29
7(d). Same as Figure 7(a), but for an energy flux threshold of 60 kR.	30
A-1. Days 1 -31.	34
A-2. Days 31 - 61.	35
A-3. Days 61 - 91.	36

List of Figures (cont'd)

<u>Figure</u>	<u>Page</u>
A-4. Days 91 - 121.	37
A-5. Days 121 - 152.	38
A-6. Days 152 - 182.	39
A-7. Days 182 - 212.	40
A-8. Days 212 - 242.	41
A-9. Days 242 - 272.	42
A-10. Days 272 - 302.	43
A-11. Days 302 - 332.	44
A-12. Days 332 - 362.	45
A-13. Days 362 - 372.	46

LIST OF TABLES

<u>Table</u>	<u>Page</u>
1. Kp and Electron Events Characteristics	4

ACKNOWLEDGEMENTS

We thank Dr. D. A. Hardy for numerous discussions on many aspects of the DMSP flux measurements in general, and in particular, on the relation of intense fluxes of precipitating electrons to geomagnetic activity. We are also appreciative of our colleague Nelson A. Bonito's efforts in overseeing this project.

1.0 INTRODUCTION

This study is to determine the dependence of the auroral DMSP electron precipitation events upon the geomagnetic Kp index. Using known values of Kp, this study determines the average number of occurrences of auroral events of varying intensity. These auroral events are defined by an electron energy flux (JETot) that exceeds specified threshold values.

To study the relationship between the auroral DMSP electron precipitation events and the geomagnetic Kp index, the superposed epoch analysis technique was implemented. This approach was used by Nagai in determining the relationship between several geomagnetic indices [Nagai, 1988]. Epoch zero is the time at which Kp values persisted above a specified threshold value for a specified duration. The zero epochs are determined from the available data, and the Kp series are superposed over a time window ranging from one day before the zero epoch to three days after. The superposed Kp series are then averaged over all epochs. The same procedure is used to obtain the corresponding time series of electron auroral events for comparison with the Kp index.

It is important to note that the results from this study cannot be used to locate these auroral events spatially. Estimating the location of these events was done in a separate study on the same DMSP data [Bounar and Hardy, 1992]. The present study can be used to estimate the auroral activity based on the geomagnetic activity.

In the next section, we describe the approach taken in generating the data base over each hemispheric pass. We then discuss the Kp index and the number of events as a function of the Kp threshold and Kp persistence values. We end this report with some suggestions for further studies that can be very beneficial in understanding the auroral activity temporal variations.

2.0 DATA BASE GENERATION

The data base was generated by processing the DMSP/F9 electron precipitation for the year 1990. The satellite is in a circular polar orbit, in the 10:30 to 22:30 meridian, and at about 840 km altitude. The electron measurements are binned into four electron flux ranges and the magnetic activity Kp value stored for each hemispheric pass. The electron events considered are those with average energy exceeding 1 KeV. The four energy flux bins correspond roughly to brightness levels of 2kR, 6kR, 20kR, and 60kR. Note that the electron fluxes were recorded in KeV/(cm²-sec-ster) and are converted to kilo-Rayleighs (kR) using a 3969 Å spectral line emission [Figures 12-19, Chapter 12, Jursa, 1985].

In Figure 1, the Kp values observed in the first 30 days in 1990 and the corresponding electron events are shown as a function of time in days. A quick examination of these curves reveals a definite correlation between the geomagnetic index Kp and the number of electron events that are observed over several hemispheric passes. A complete set of figures of the Kp values and the number of precipitating electron events in 1990 is provided in Appendix A.

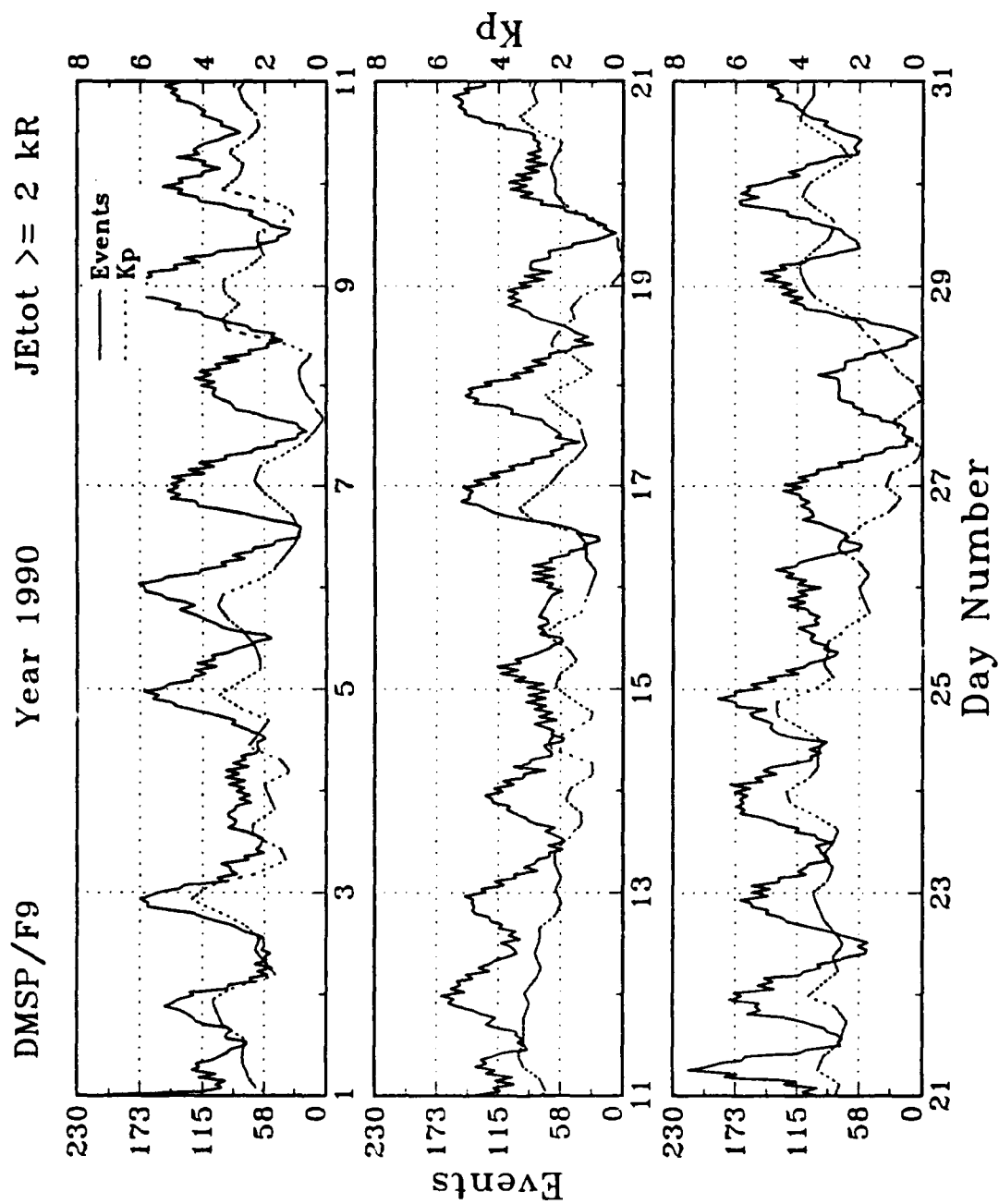


Figure 1. Kp index and number of auroral events with energy fluxes greater than or equal to 2 kR observed in each hemispheric pass. These data are based on DMSP/F9 flux measurements in 1990.

3.0 APPROACH

For a given Kp threshold value (KTH) and a specified persistence time over this threshold (KPT), the data base is scanned and the times at which these Kp conditions are satisfied are determined. These times are taken as zero epochs. That is, the time at which Kp was above the threshold value KTH for KPT hours is the zero epoch. Once an epoch is located, the scanning of the Kp data is resumed after Kp values drop below the threshold value KTH. In this way, the instances when Kp persists above KTH for over KPT hours will only be considered once. The Kp series are superposed over a time period ranging from one day before the zero epoch to three days after. The superposed Kp series are then averaged by the number of epochs. The same procedure is used to obtain the corresponding time series of electron auroral events. Note that the samples from the data base are not available at uniform intervals. Each sample represents one hemispheric pass in time; which spans about 51 minutes. This means that there is on average one hemispheric pass per hour. In other words, there is one data sample per hour. Sometimes data gaps occur so that no measurements are available for a few hours. In this analysis, the original data samples per hemispheric pass were interpolated (when gaps occurred) or averaged (when more than one sample is available) as necessary to obtain samples at every 1.2 hours.

4.0 DISCUSSION OF THE RESULTS

Some of the results are summarized in the Table 1. The columns 1 through 6 give Kp parameters, which are the Kp persistence in hours (PKT in column 1) above a specified Kp threshold value (KTH in column 2), the Kp peak value (KPP in column 3) and its time of occurrence (KTP in column 4), the rise time of Kp from the threshold value to the peak value (ΔRT in column 5), and the fall time from the peak value to the threshold value (ΔFT in column 6). The remaining columns give information on the maxima of the number of occurrences of electron events and their time of occurrence for a JEtot threshold of 2 kR (#Ev and time in columns 7 and 8, respectively), for a JEtot threshold of 6 kR (columns 9 and 10, respectively), for a JEtot threshold of 20 kR (columns 11 and 12, respectively), for a JEtot threshold of 60 kR (columns 13 and 14, respectively).

Whenever a rise or a fall time is larger than the time window available, it is denoted by asterisks. Whenever a time of occurrence is unreliable because of poor statistics, a question mark is appended to its value. Note that a negative time for the occurrence of a peak means that it occurred before epoch zero.

Table 1. Kp and Electron Events Characteristics													
Kp Peak, Rise and Fall Times						JEtot ≥ 2 kR <Ev> = 62.6		JEtot ≥ 6 kR <Ev> = 22.8		JEtot ≥ 20 kR <Ev> = 6.8		JEtot ≥ 60 kR <Ev> = 2.8	
PKT	KTH	KPP	KTP	ΔRT	ΔFT	#Ev	Time	#Ev	Time	#Ev	Time	#Ev	Time
3	2.0	2.7	-1.2	2.4	*****	75.0	.0	24.7	0.0	7.1	69.67	2.9	42.07
3	2.5	3.3	-1.2	2.4	34.8	86.1	-1.2	31.0	-1.2	8.4	1.2	3.3	42.07
3	3.0	3.8	-1.2	2.4	16.8	97.5	-1.2	38.1	-1.2	10.2	.0	3.7	1.2
3	3.5	4.4	-1.2	2.4	9.6	98.9	-1.2	43.3	-2.4	11.9	-1.2	3.6	10.87
3	4.0	4.9	-1.2	2.4	4.8	96.1	-1.2	48.4	-2.4	14.1	-2.4	4.4	6.07
3	4.5	5.5	-2.4	1.2	4.8	99.4	-1.2	48.5	-2.4	15.3	-1.2	4.9	2.4
3	5.0	5.9	-2.4	1.2	8.4	101.8	-1.2	46.7	-3.6	16.3	-2.4	6.0	1.2
6	2.0	2.9	-2.4	4.8	*****	77.2	-3.6	27.1	1.2	7.1	67.27	3.0	2.4
6	2.5	3.7	-2.4	4.8	51.6	93.4	.0	36.7	-3.6	9.5	-1.2	3.5	42.07
6	3.0	4.1	-2.4	4.8	26.4	97.4	-3.6	40.9	-1.2	11.0	-2.4	3.7	-2.4
6	3.5	4.8	-2.4	4.8	14.4	98.4	-3.6	42.3	-6.0	12.2	-6.0	3.8	6.07
6	4.0	5.2	-3.6	3.6	13.2	105.3	-3.6	47.8	-4.8	15.9	-6.0	4.6	1.2
6	4.5	5.7	-3.6	3.6	8.4	106.6	-3.6	52.0	-1.2	17.0	-6.0	5.2	1.2
6	5.0	6.3	-2.4	4.8	6.0	104.6	-4.8	55.1	-6.0	19.7	1.2	6.7	.0
9	2.0	3.1	-1.2	8.4	*****	79.0	-1.2	28.9	-1.2	7.8	31.27	2.9	64.87
9	2.5	3.9	-2.4	7.2	57.6	96.1	-2.4	39.0	-2.4	10.3	-3.6	3.5	43.27
9	3.0	4.2	-3.6	6.0	28.8	98.2	-6.0	40.3	-3.6	10.9	-3.6	3.8	-4.8
9	3.5	5.0	-3.6	6.0	13.2	98.4	-6.0	43.8	-1.2	11.9	-4.8	3.9	2.4
9	4.0	5.4	-3.6	6.0	10.8	102.0	-6.0	53.1	-8.4	16.3	-8.4	4.7	1.2
9	4.5	6.1	-3.6	6.0	10.8	108.2	-7.2	58.5	-2.4	17.8	-1.2	5.5	-1.2
9	5.0	6.3	-4.8	4.8	7.2	107.7	-7.2	60.6	-3.6	18.7	-2.4	6.1	-1.2
12	2.0	3.3	-3.6	9.6	*****	83.9	1.2	29.8	-4.8	8.1	12.0	3.1	58.87
12	2.5	4.0	-6.0	7.2	64.8	96.5	-4.8	38.5	-6.0	9.4	-8.4	3.7	1.2
12	3.0	4.4	-6.0	7.2	30.0	97.9	-8.4	40.5	-7.2	11.3	-10.8	3.7	27.67
12	3.5	5.1	-6.0	7.2	27.6	100.9	-1.2	51.6	-4.8	12.6	-1.2	5.0	1.2
12	4.0	5.7	-6.0	8.4	15.6	102.7	-4.8	57.6	-3.6	17.5	-3.6	4.8	-2.4
12	4.5	6.2	-7.2	7.2	12.0	113.6	-10.8	62.6	-6.0	16.4	-4.8	4.6	-6.0
12	5.0	6.8	-3.6	9.6	10.8	105.0	-10.8	64.7	-7.2	20.3	-4.8	6.0	-6.0

All the figures of Kp and the number of events are shown with respect to time away from epoch zero. These values are shown uniformly in time at every 1.2 hours even though the processed DMSP data is based on hemispheric passes that do not occur uniformly.

The results reveal certain properties: (1) The peak values in Kp and the number of events increase with increasing Kp threshold values. (2) The spread or the width of the Kp values above the Kp threshold value increases with increasing Kp threshold value. (3) The spread or the dispersion of the number of events above the mean increases with increasing Kp thresholds, but stays unchanged with increasing Kp persistence time. (4) The peak of the number of events tends to occur at the same time or a few hours later than the Kp peak. (5) The peak of the number of events increases sharply when the Kp thresholds are increased beyond the mean Kp value, and then levels off for Kp thresholds greater than the mean Kp value plus 1.0.

4.1 Kp CHARACTERISTICS

We first discuss certain characteristics of the geomagnetic index Kp as the Kp threshold and persistence time is varied. These conclusions are drawn from Figure 2, and are summarized in Table 1. For a Kp threshold of 3.0, and a persistence time of at least 3 hours (Figure 2a), a negative bias in the Kp peak of about 1.2 hours is observed. This bias increases in magnitude as the persistence time is increased. When the persistence time is 12 hours, this bias is as much as 6.0 hours (Figure 2d).

The Kp peak values increase with increasing Kp thresholds. For a Kp threshold of 4.0, the Kp peak is 4.9 when the persistence time is 3.0, and is 5.4 when the persistence time is increased to 9 hours (Figures 2a and 2c). One reason for this increase is the fact that the more disturbed the geomagnetic activities, the longer they persist.

The Kp rise time from the Kp threshold to the Kp peak value is generally smaller for higher Kp thresholds. For a persistence time of 3 hours and a Kp threshold of 3.0, the rise time is 2.4 hours (Figure 2a). When the threshold is increased to 5.0, the rise time drops to 1.2 hours. Furthermore, a shorter Kp rise time generally leads to a shorter Kp fall time. The Kp fall time is the time it takes Kp to drop from the peak value to the threshold value. For the same Kp persistence value, the fall time is 16.8 hours for a Kp threshold of 3.0, and is 8.4 hours for a Kp threshold of 5.0. Another important feature of Kp is how the rise time and fall time relate. For a persistence time of 3 hours, the fall time is at least twice as long as the rise time. This ratio drops to slightly above one when the persistence time is increased.

4.2 ELECTRON EVENTS CHARACTERISTICS

The characteristics of the number of events as the Kp threshold and persistence time is varied are discussed below. These conclusions are drawn from Table 1 and Figures 3 through 7. Consider first events with JEtot exceeding 2 kR. The peak value of the number of events increases as the Kp threshold increase. For a persistence time of 3 hours (Figure 3a), 98 events are observed for a Kp threshold of

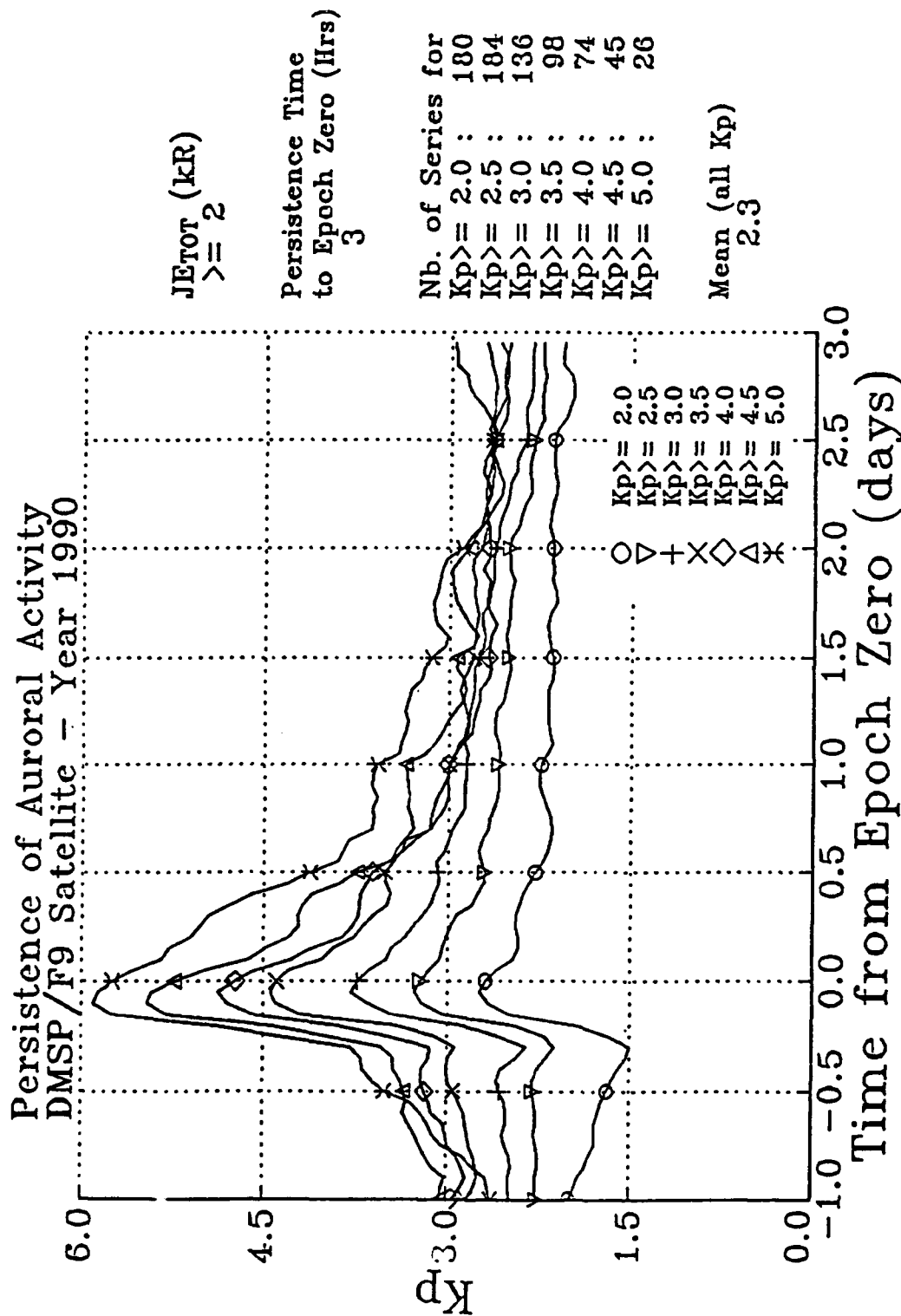


Figure 2(a). Superposed epochs of Kp index over a time window of 4 days with a sampling rate of 1.2 hours. Seven curves are plotted, each corresponding to a different Kp threshold. This figure is for a Kp persistence time of 3 hours.

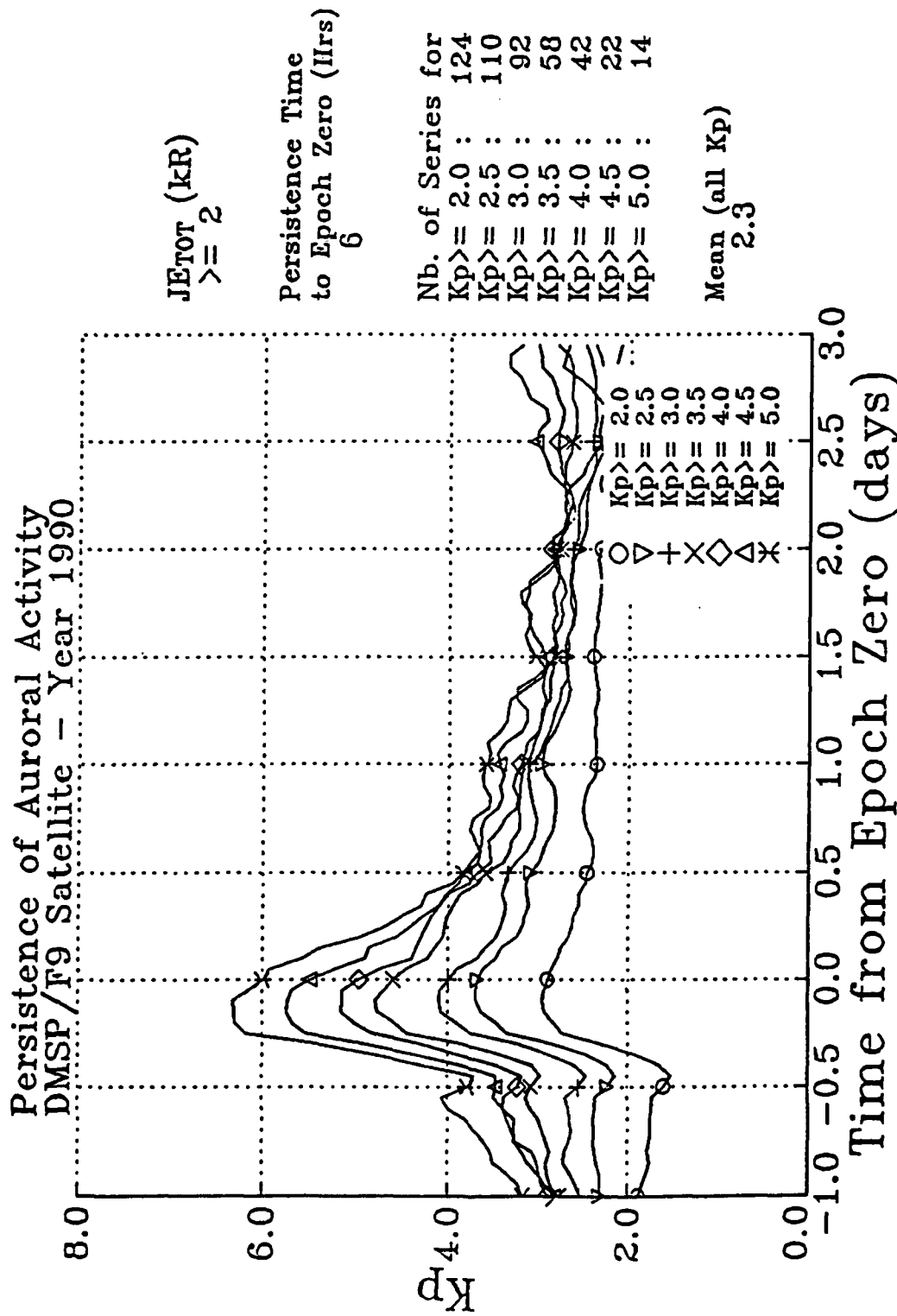


Figure 2(b). Same as Figure 2(a), but for a Kp persistence time of 6 hours.

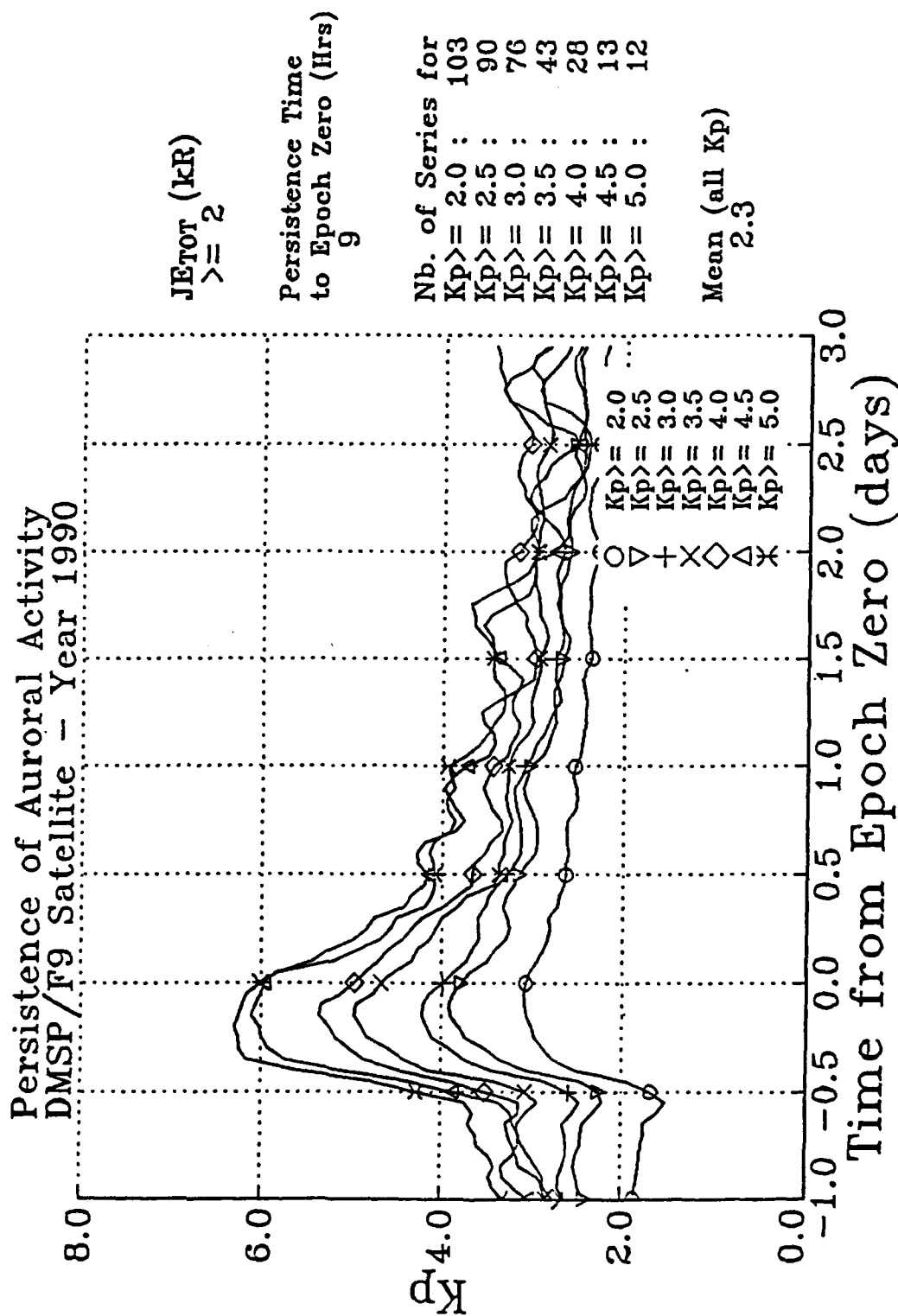


Figure 2(c). Same as Figure 2(a), but for a Kp persistence time of 9 hours.

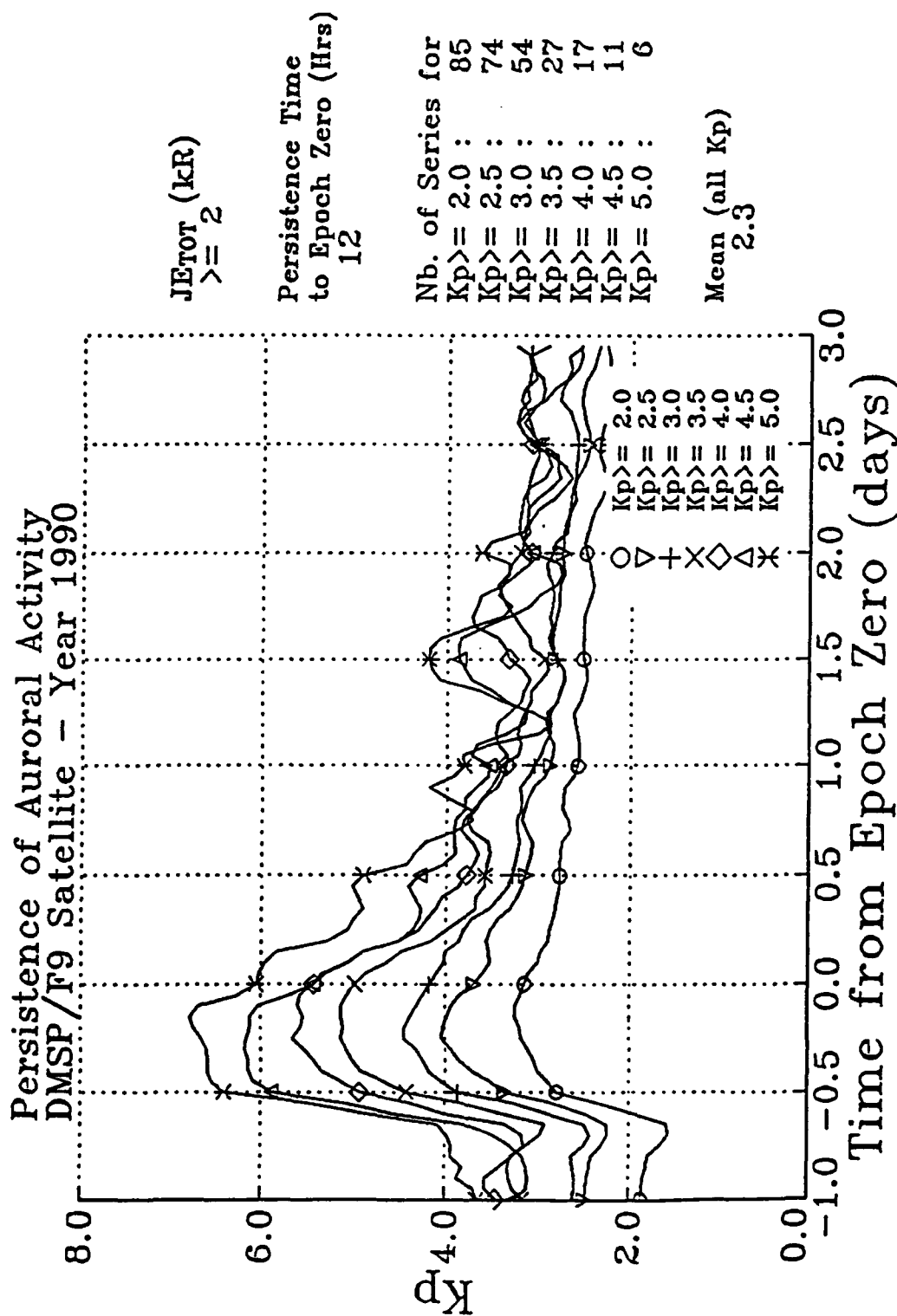


Figure 2(d). Same as Figure 2(a), but for a K_p persistence time of 12 hours.

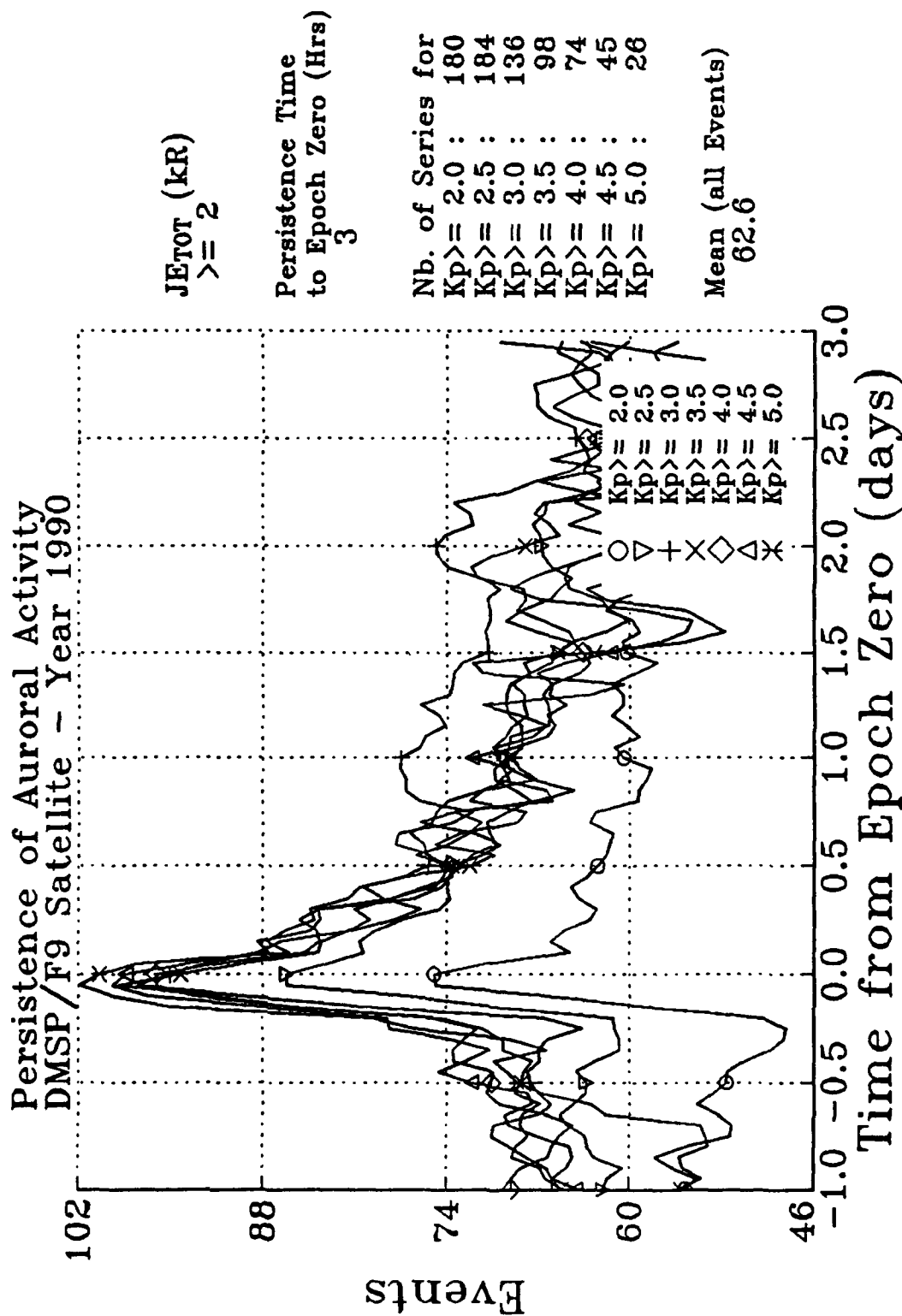


Figure 3(a). Superposed epochs of the number of events per hemispheric pass for energy fluxes (J_{ETOT}) greater than or equal to 2 kR over a time window of 4 days with a sampling rate of 1.2 hours. Seven curves are plotted, each corresponding to a different Kp threshold (same as Figure 2). This figure is for a Kp persistence time of 3 hours.

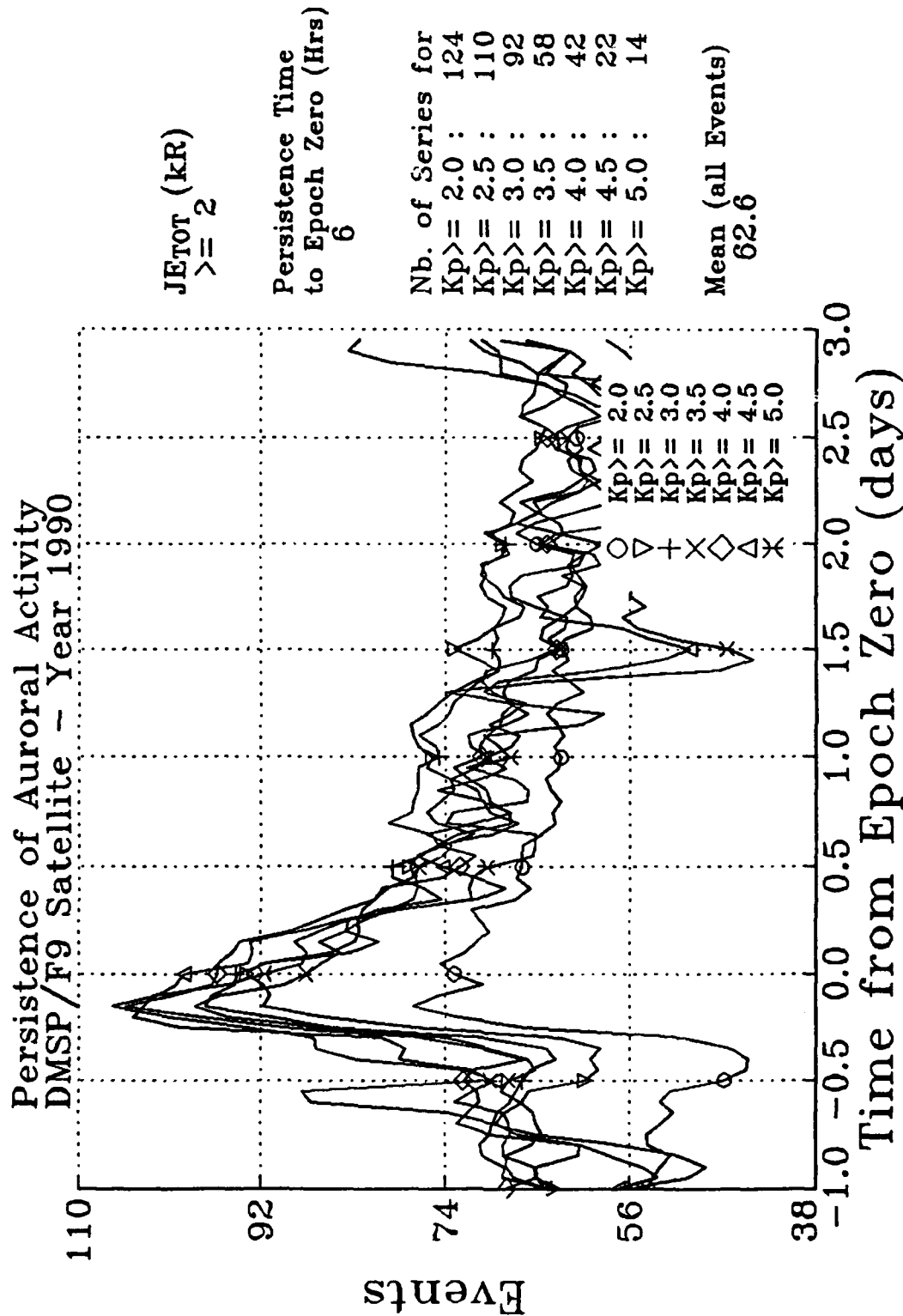


Figure 3(b). Same as Figure 3(a), but for a Kp persistence time of 6 hours.

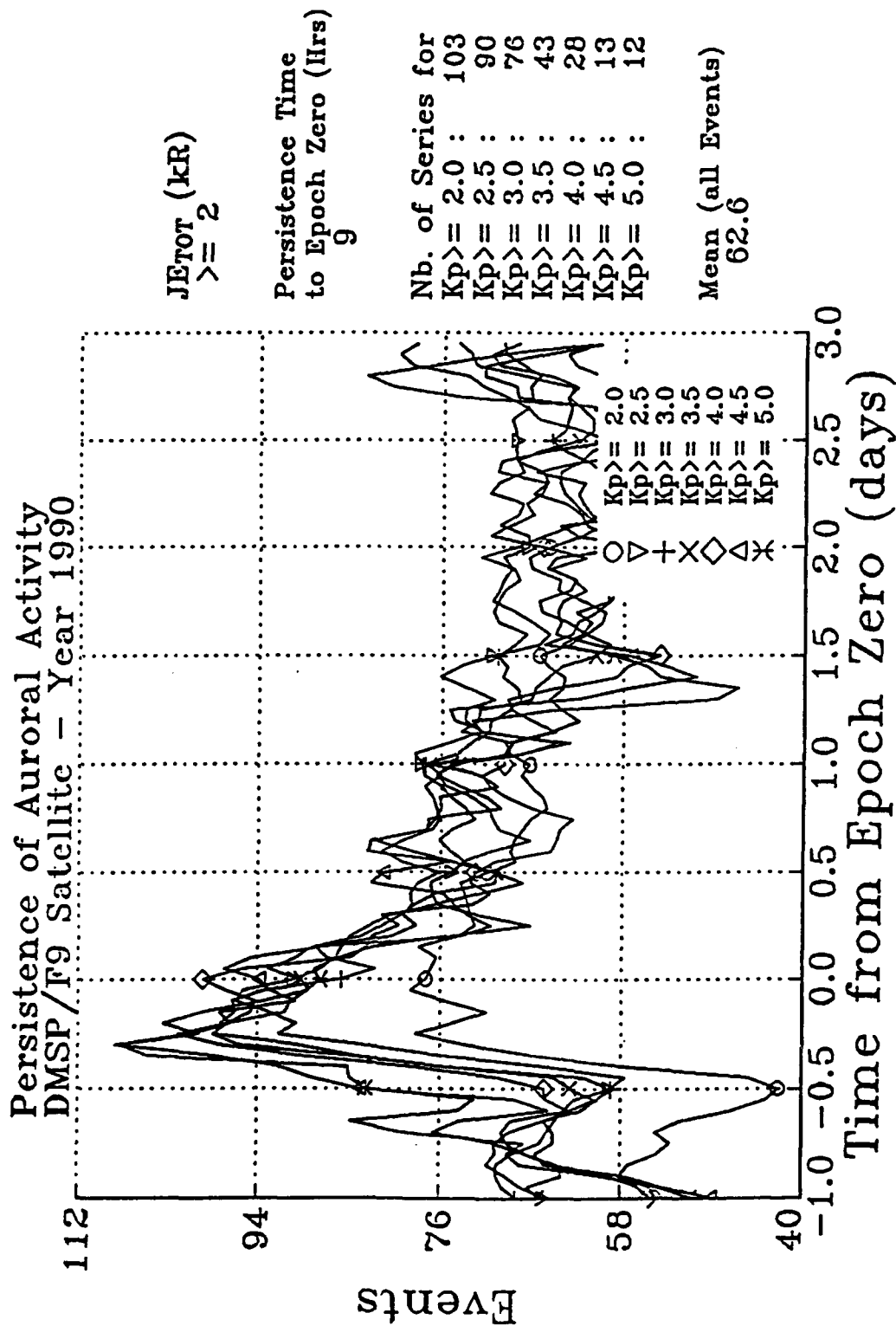


Figure 3(c). Same as Figure 3(a), but for a Kp persistence time of 9 hours.

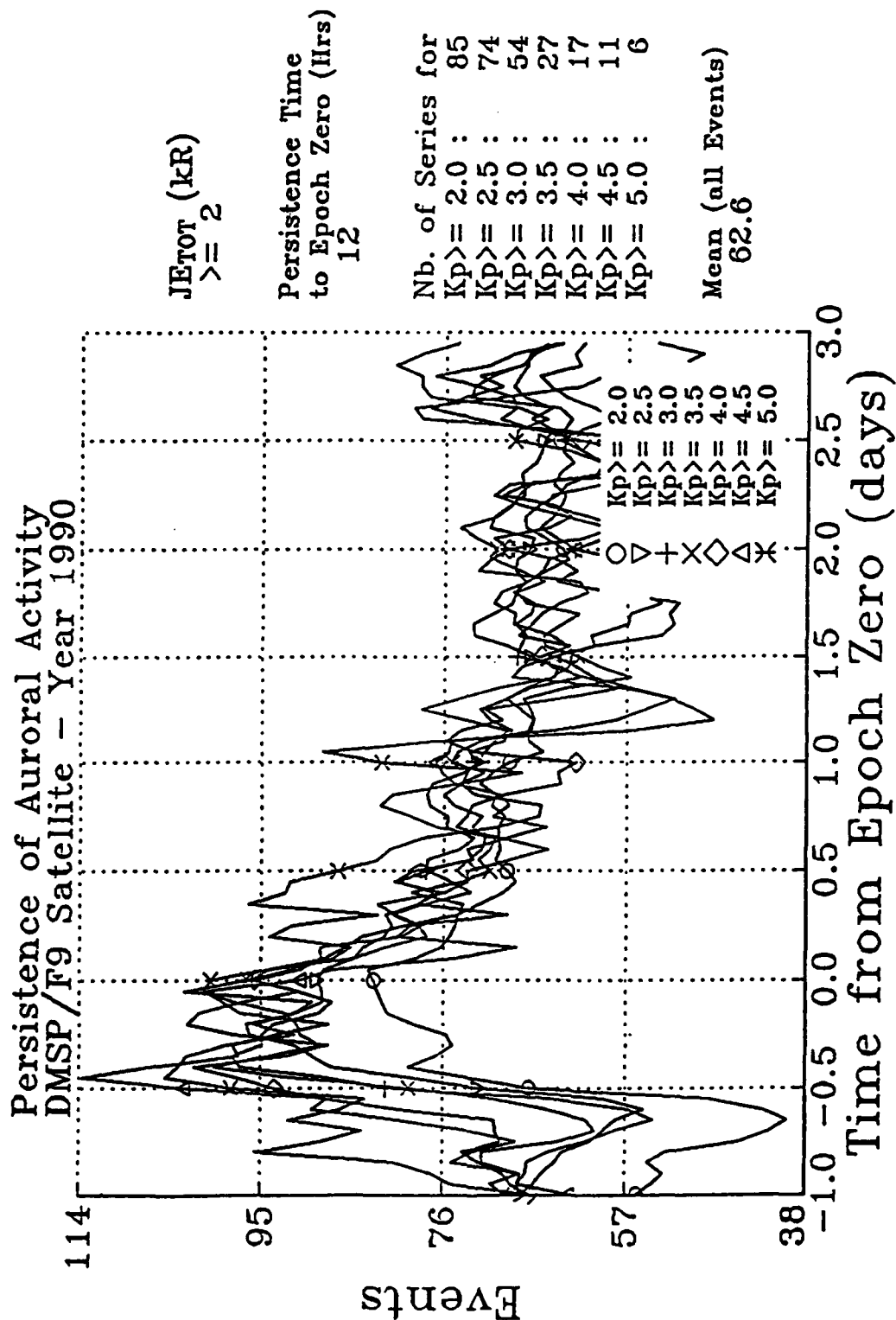


Figure 3(d). Same as Figure 3(a), but for a Kp persistence time of 12 hours.

3 as opposed to 102 events for a Kp threshold of 5. The mean value of the number of events observed over all hemispheric passes is 63 events. The peak of the number of events increases sharply when the Kp thresholds are increased beyond the mean Kp value, and then levels off for Kp thresholds greater than the mean Kp value plus 1.0. For a persistence time of 3 hours (Figure 3a) and for Kp threshold values not exceeding Kp mean of 2.3, the peak value increased by about 11 events each time the Kp threshold was increased by $\frac{1}{2}$. For Kp thresholds greater than or equal to 3.0, the peak variation increases by only 2 events for every Kp threshold increase of $\frac{1}{2}$.

The fall time for the number of events is at least twice as long as the rise time. For instance, for a persistence value of 3 hours (Figure 3a), and a Kp threshold of 5.0, the rise time is 13 hours and the fall time is 32 hours. The change in this ratio is very small and hence negligible as the persistence time is increased (see Figures 3b through 3d).

Figure 4 shows results of events with JEtot exceeding 6 kR. The peak value of the number of events increases as the Kp threshold increases. For a persistence of 3 hours (Figure 4a), 38 events are observed for a Kp threshold of 3 as opposed to 47 events for a Kp threshold of 5. The mean value of the number of events observed over all hemispheric passes is 23 events.

The fall time for the number of events is at least twice as long as the rise time. For instance, for a persistence value of 3 hours (Figure 4a), and a Kp threshold of 5.0, the rise time is 12 hours and the fall time is 34 hours. The change in this ratio is very small and hence negligible as the persistence time is increased (see Figures 4b through 4d). The rise time is generally about $\frac{1}{2}$ day and the fall time varies between 1.0 and 1.5 days.

The results of events with JEtot exceeding 20 kR are shown in Figure 5. For a persistence of 3 hours (Figure 5a), 10 events are observed for a Kp threshold of 3 as opposed to 16 events for a Kp threshold of 5. The mean value of the number of events observed over all hemispheric passes is about 7 events.

Figure 6 shows results of events with JEtot exceeding 60 kR. For a persistence of 3 hours (Figure 6a), 4 events are observed for a Kp threshold of 3 as opposed to 6 events for a Kp threshold of 5. The mean value of the number of events observed over all hemispheric passes is 3 events.

4.3 COMPARISON OF Kp AND ELECTRON EVENTS

Figure 7 shows the Kp and the number of events for all five JEtot thresholds. The Kp threshold is selected at 4.0 and Kp values stay above this Kp threshold for at least 3 hours. These figures show how well correlated the number of events are with Kp. At about $\frac{1}{2}$ day before epoch zero, Kp rises very rapidly from a Kp value of 3.0 to a peak value near epoch zero, then the Kp values drop below the Kp value of 3.0 in about 1 day. These same features are seen in the number of events, with a rapid rise then a slow fall in the number of events. The rise time from the mean value to the peak value is about $\frac{1}{2}$ day and the fall time is about 1 day.

To measure the correlation between Kp and the number of events, the normalized correlation coefficient is computed for Kp above the specified threshold value. The correlation coefficient is defined as the ratio of the expected value of the product of Kp and the number of events to the product of their standard deviations. Assuming stationarity in Kp and the auroral events, the time average is used instead of

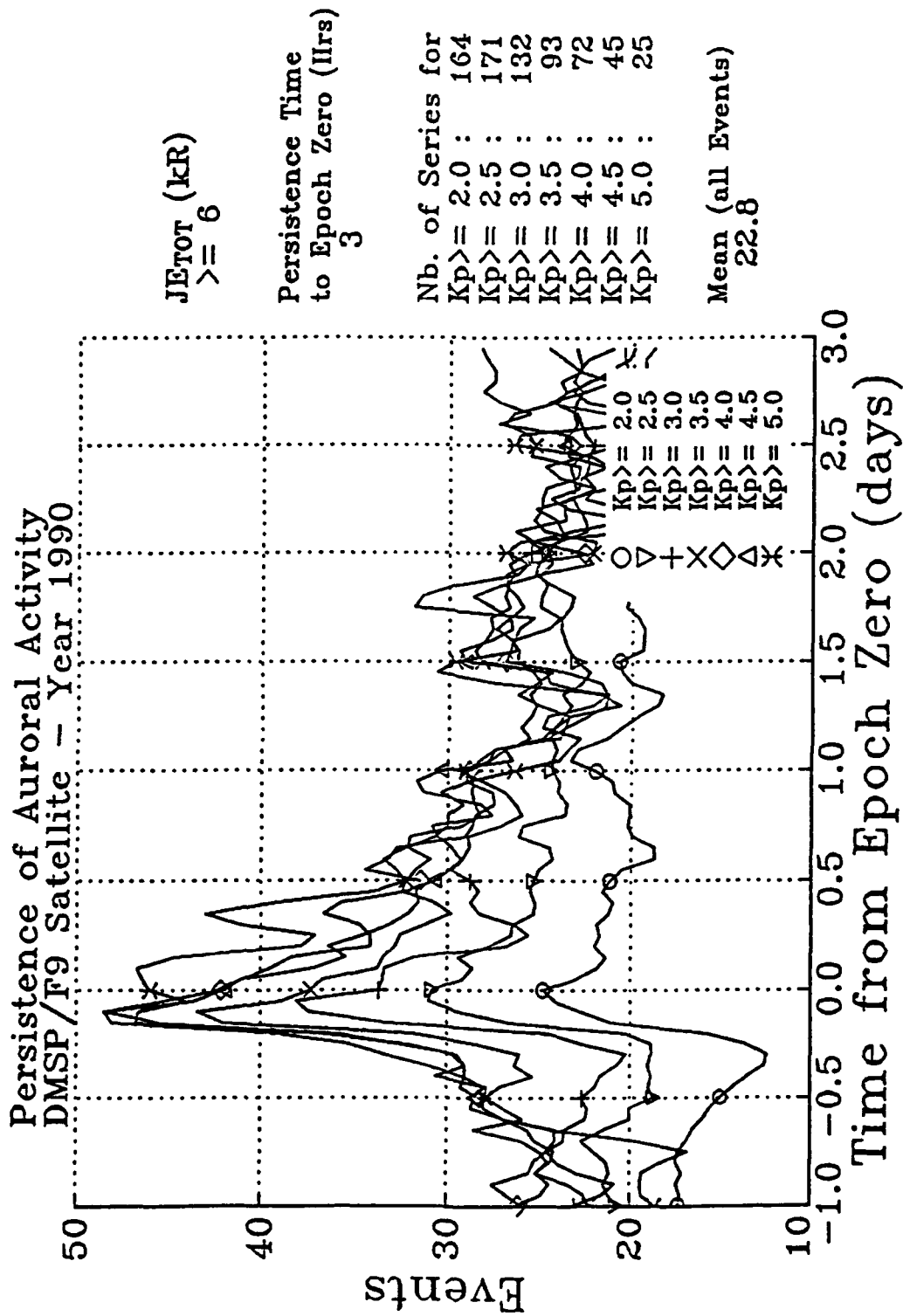


Figure 4(a). Same as Figure 3(a), except that $J_{Etot} \geq 6$ kR.

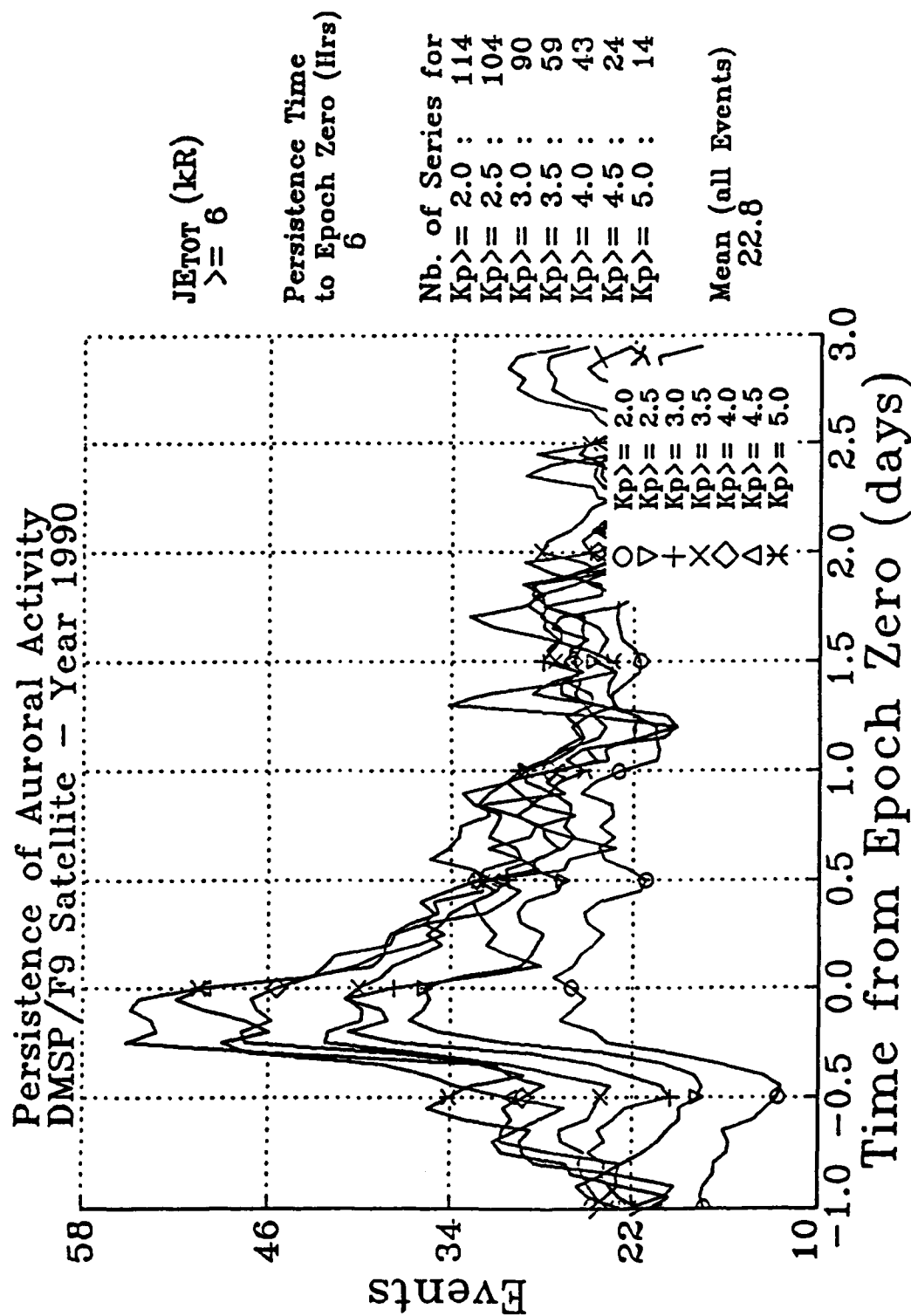


Figure 4(b). Same as Figure 3(b), except that $J_{Etot} \geq 6$ kR.

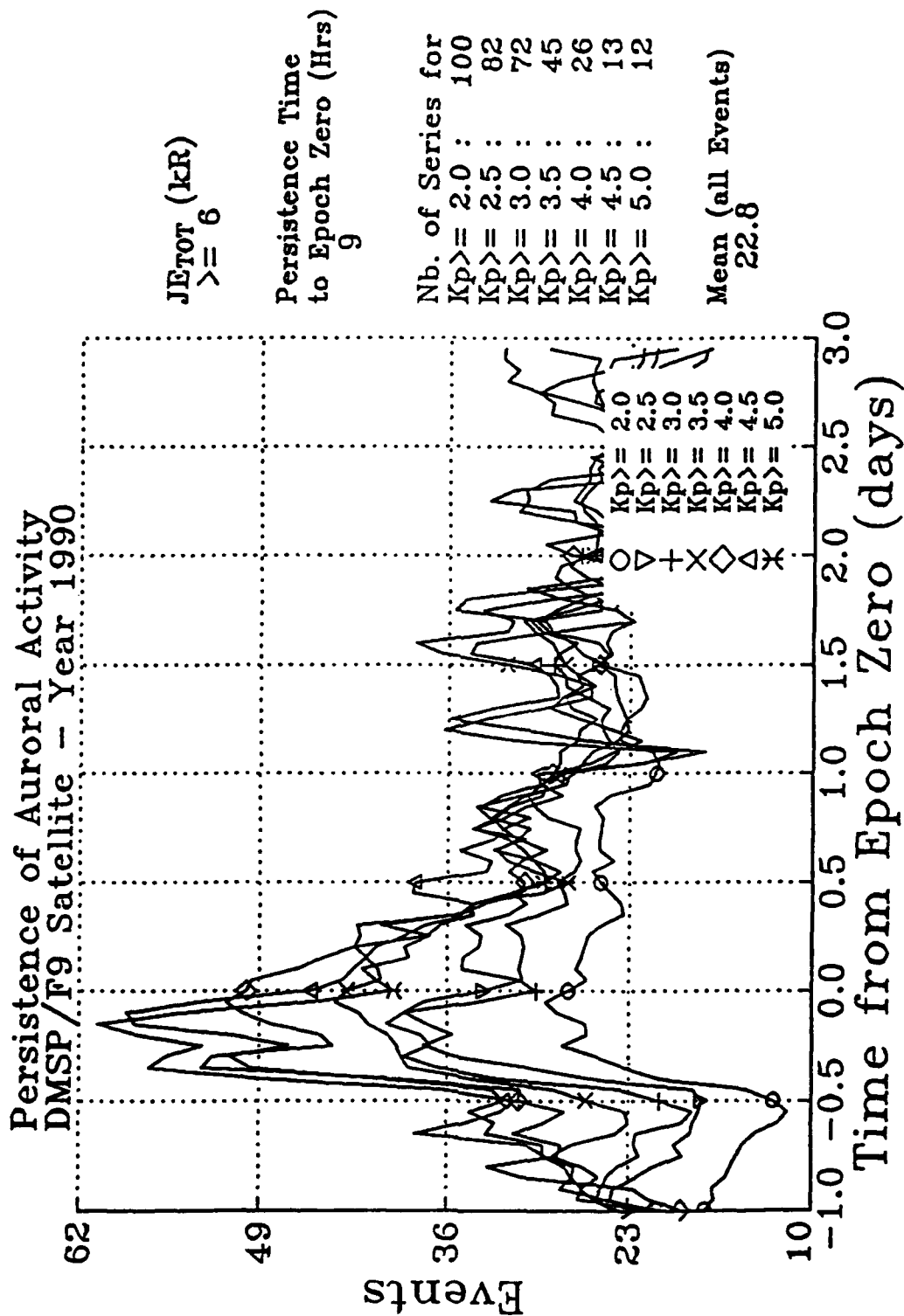


Figure 4(c). Same as Figure 3(c), except that $JE_{TOT} \geq 6$ kR.

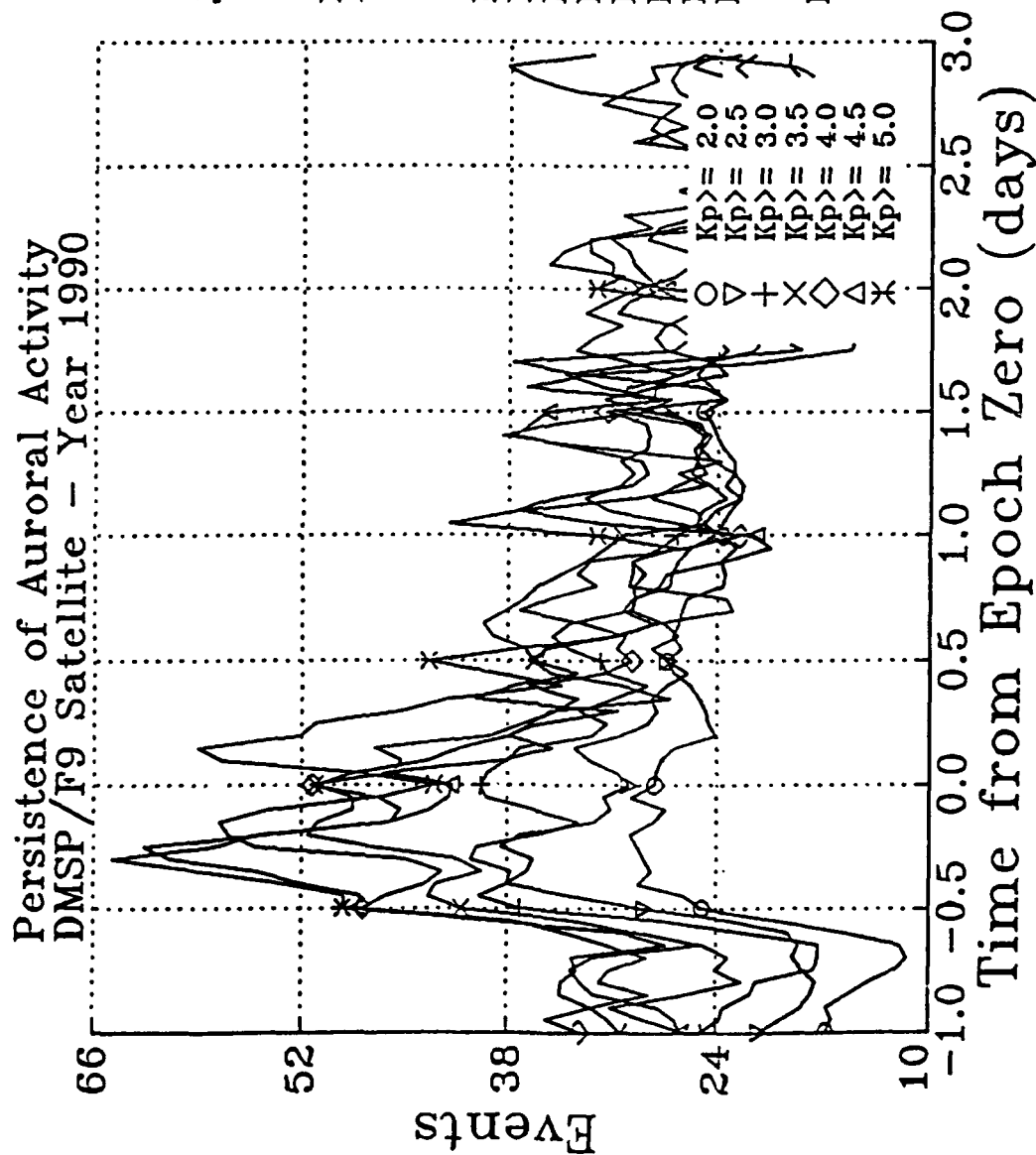


Figure 4(d). Same as Figure 3(d), except that $J_{E_{TOT}} \geq 6$ kR.

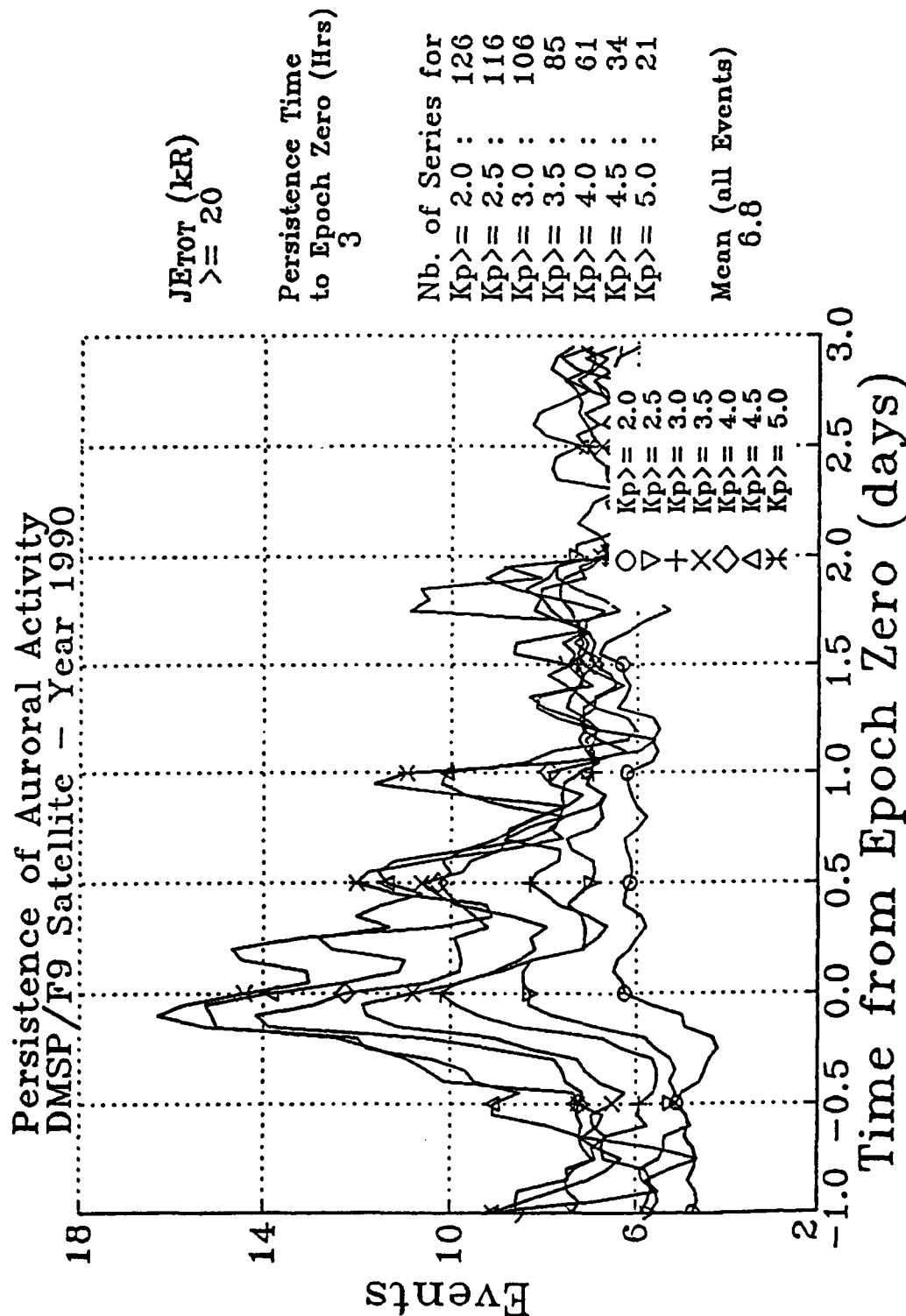


Figure 5(a). Same as Figure 3(a), except that $J_{Etot} \geq 20$ kR.

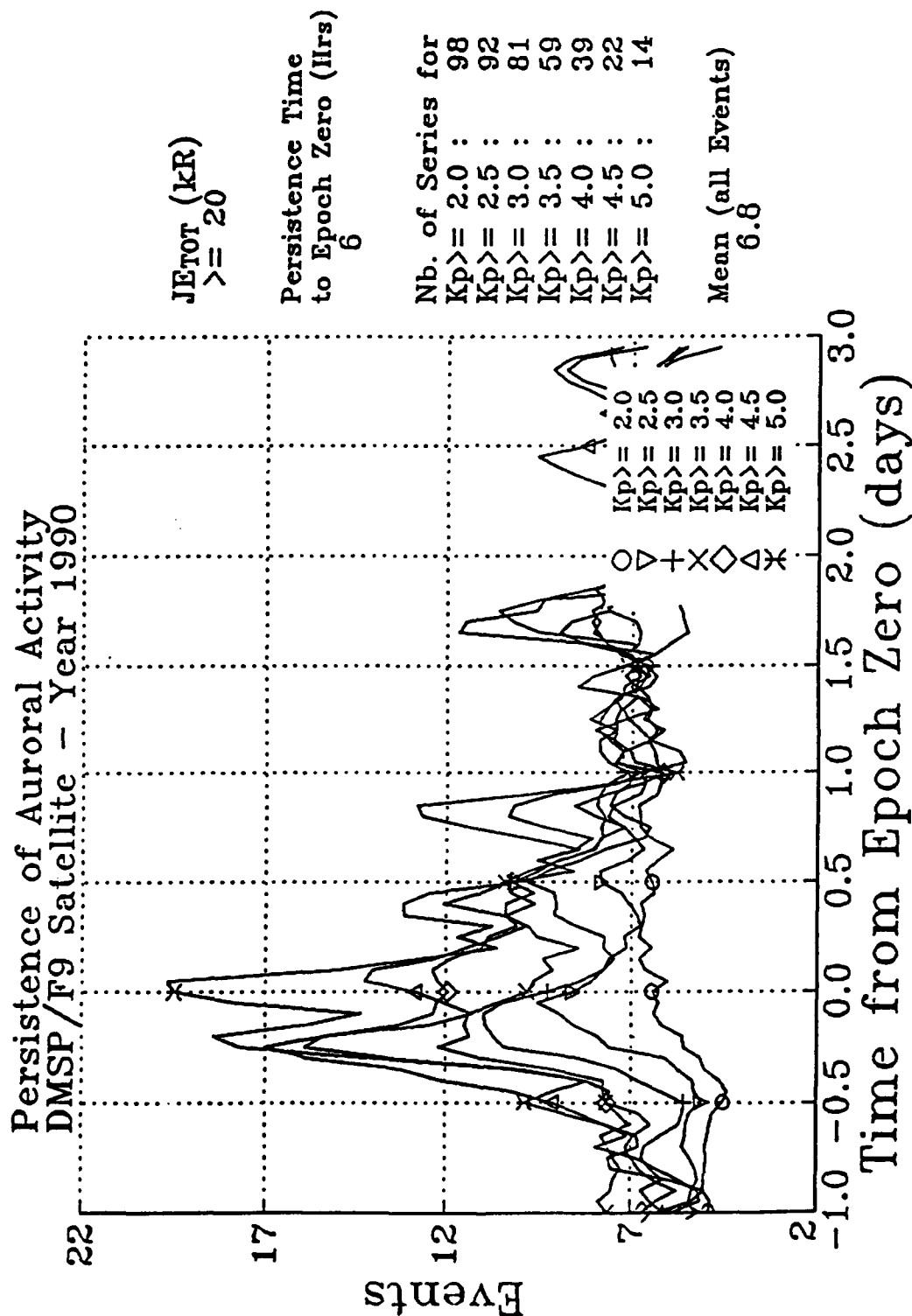


Figure 5(b). Same as Figure 3(b), except that $J_{ETOT} \geq 20$ kR.

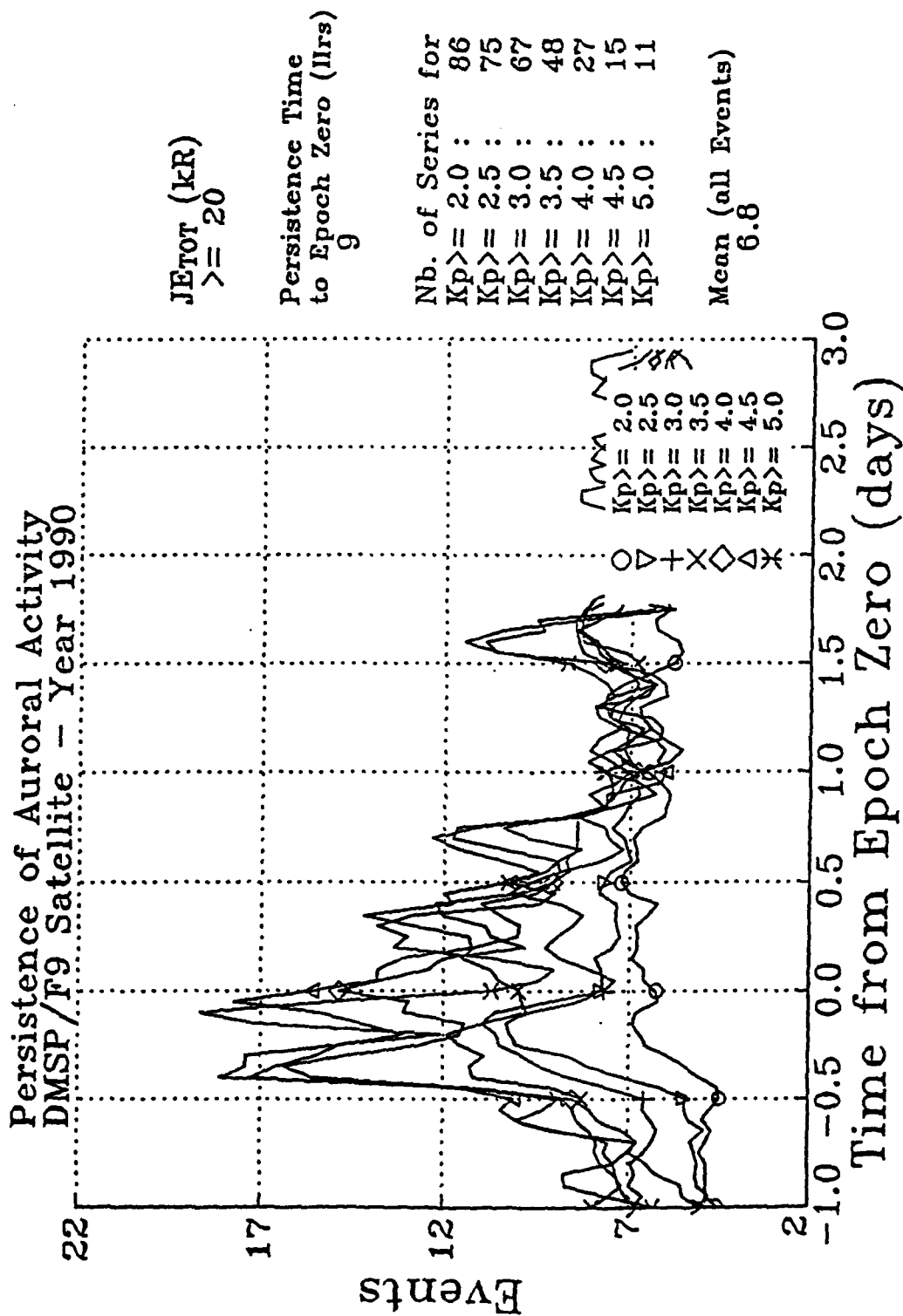


Figure 5(c). Same as Figure 3(c), except that $J_{Etot} \geq 20$ kR.

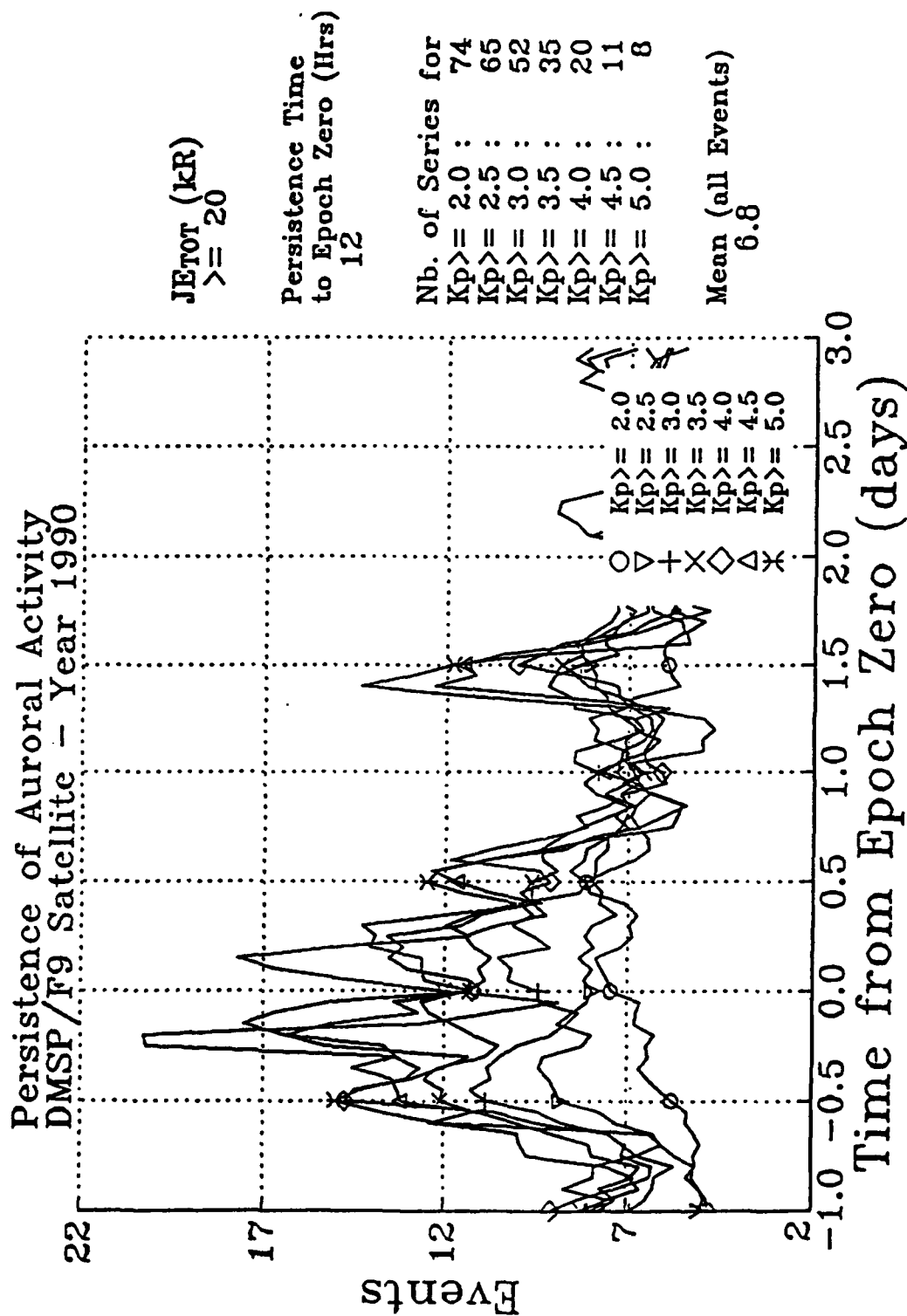


Figure 5(d). Same as Figure 3(d), except that $J_{Etot} \geq 20$ kR.

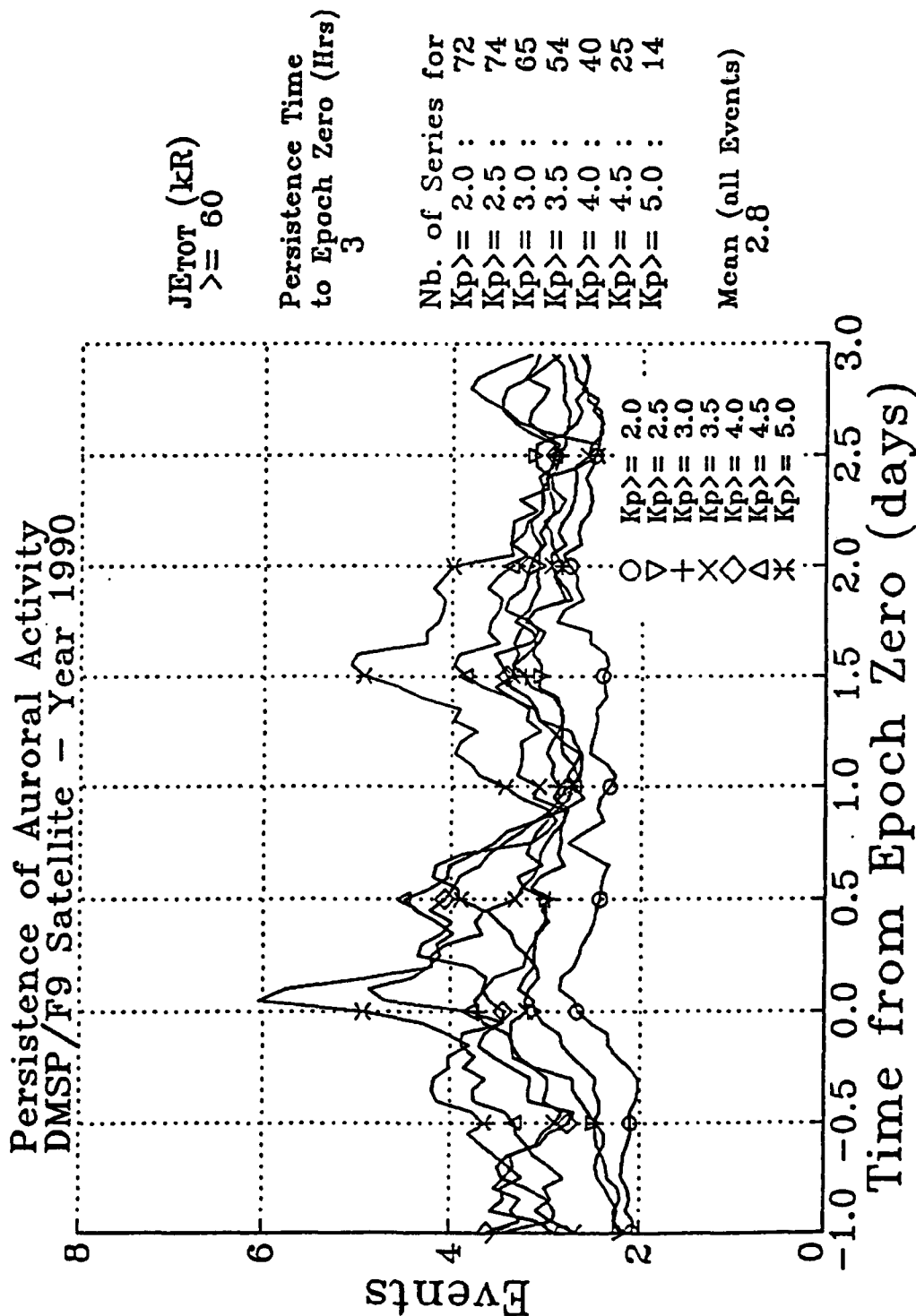


Figure 6(a). Same as Figure 3(a), except that $J_{ETOT} \geq 60$ kR.

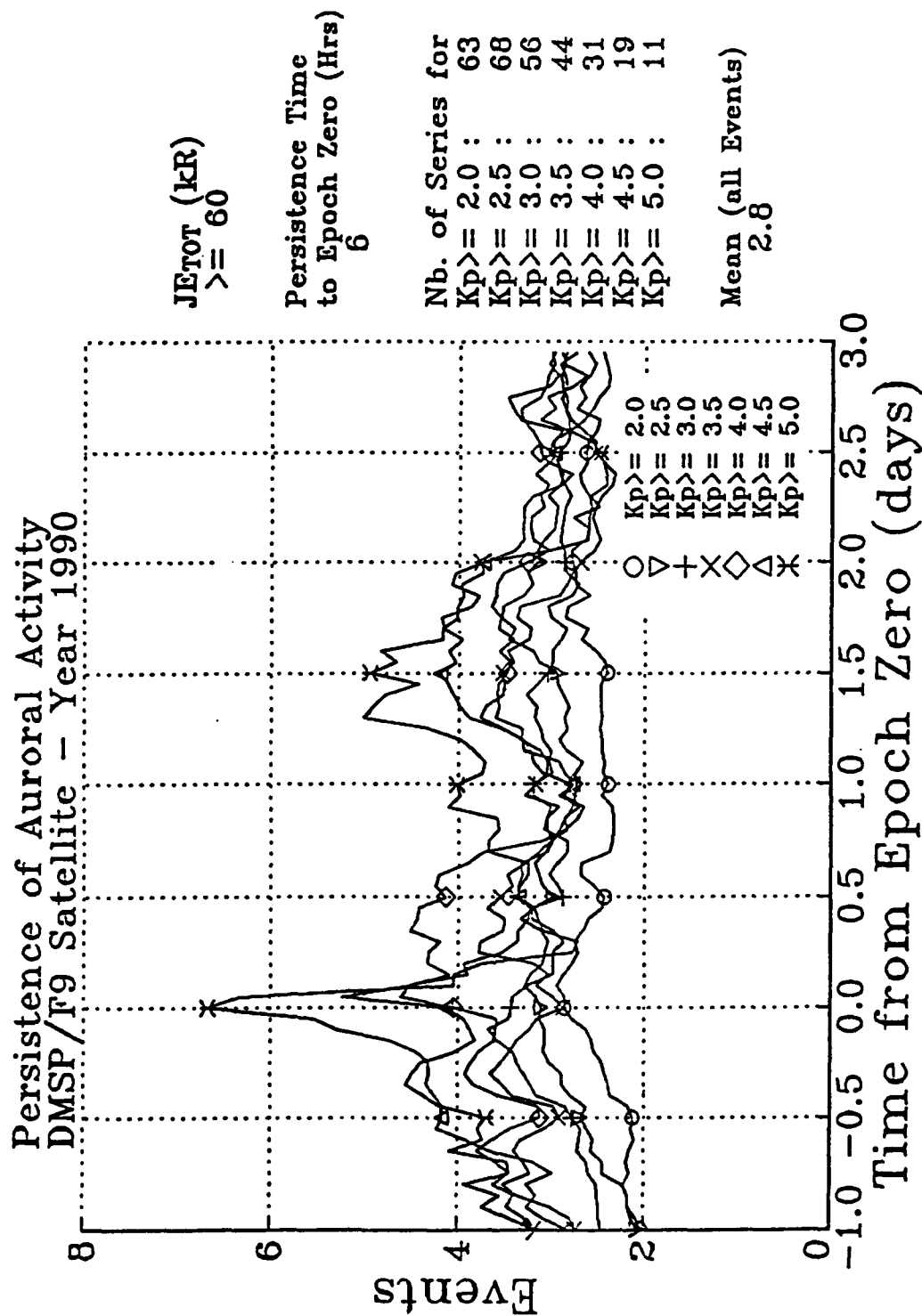


Figure 6(b). Same as Figure 3(b), except that $J_{TOT} \geq 60$ kR.

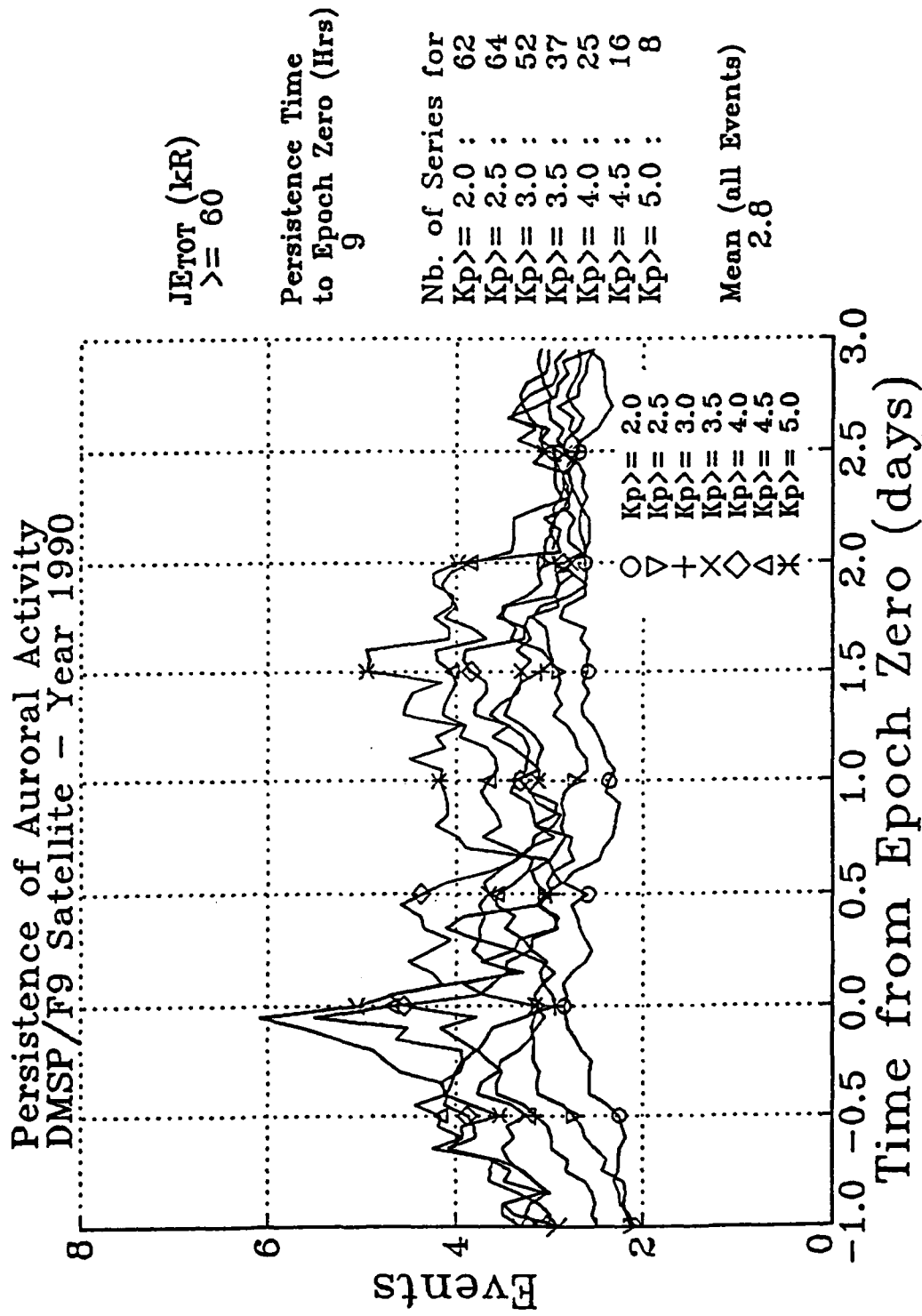
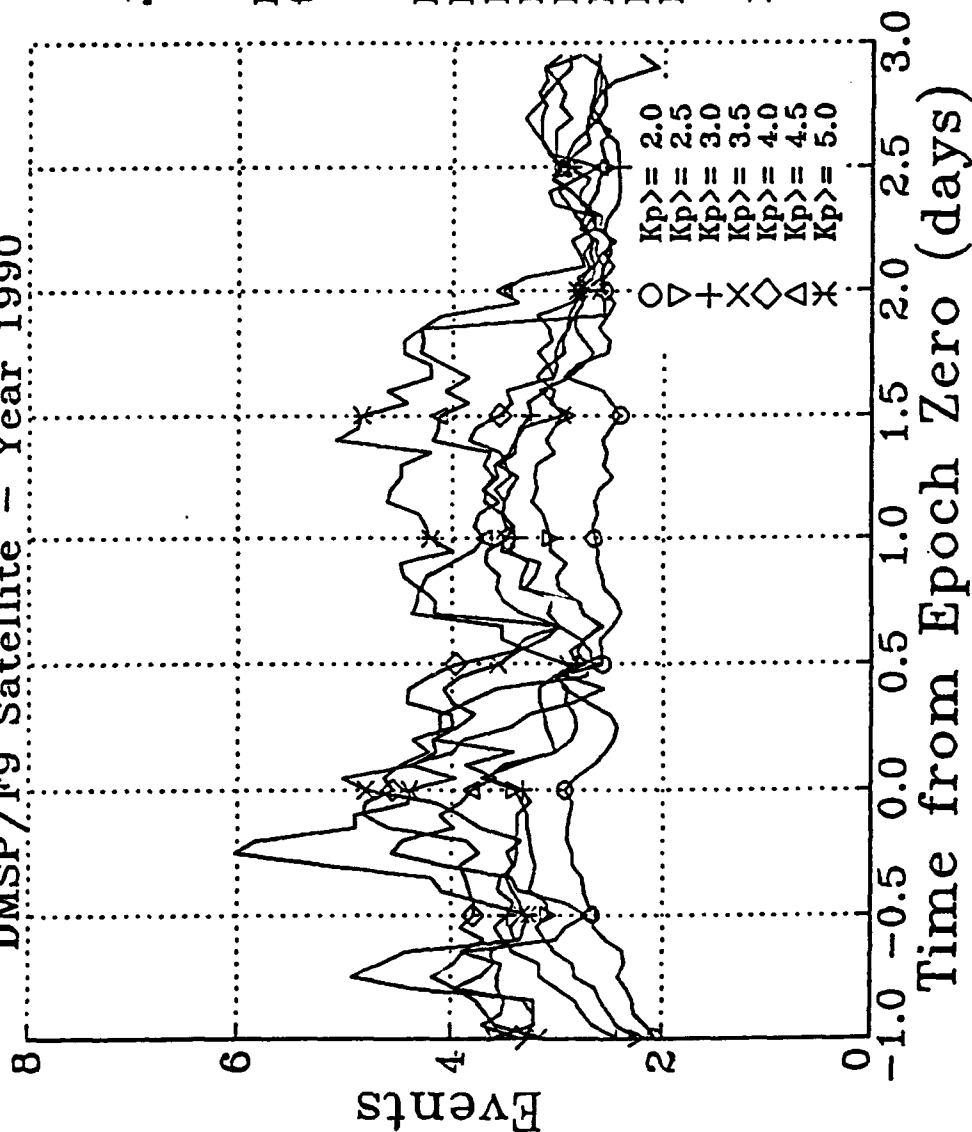


Figure 6(c). Same as Figure 3(c), except that $JE_{TOT} \geq 60$ kR.

Persistence of Auroral Activity DMSP/F9 Satellite - Year 1990



$J_{ETOT} (kR)$
 ≥ 60

Persistence Time
to Epoch Zero (Hrs)
12

Figure 6(d). Same as Figure 3(d), except that $J_{ETOT} \geq 60$ kR.

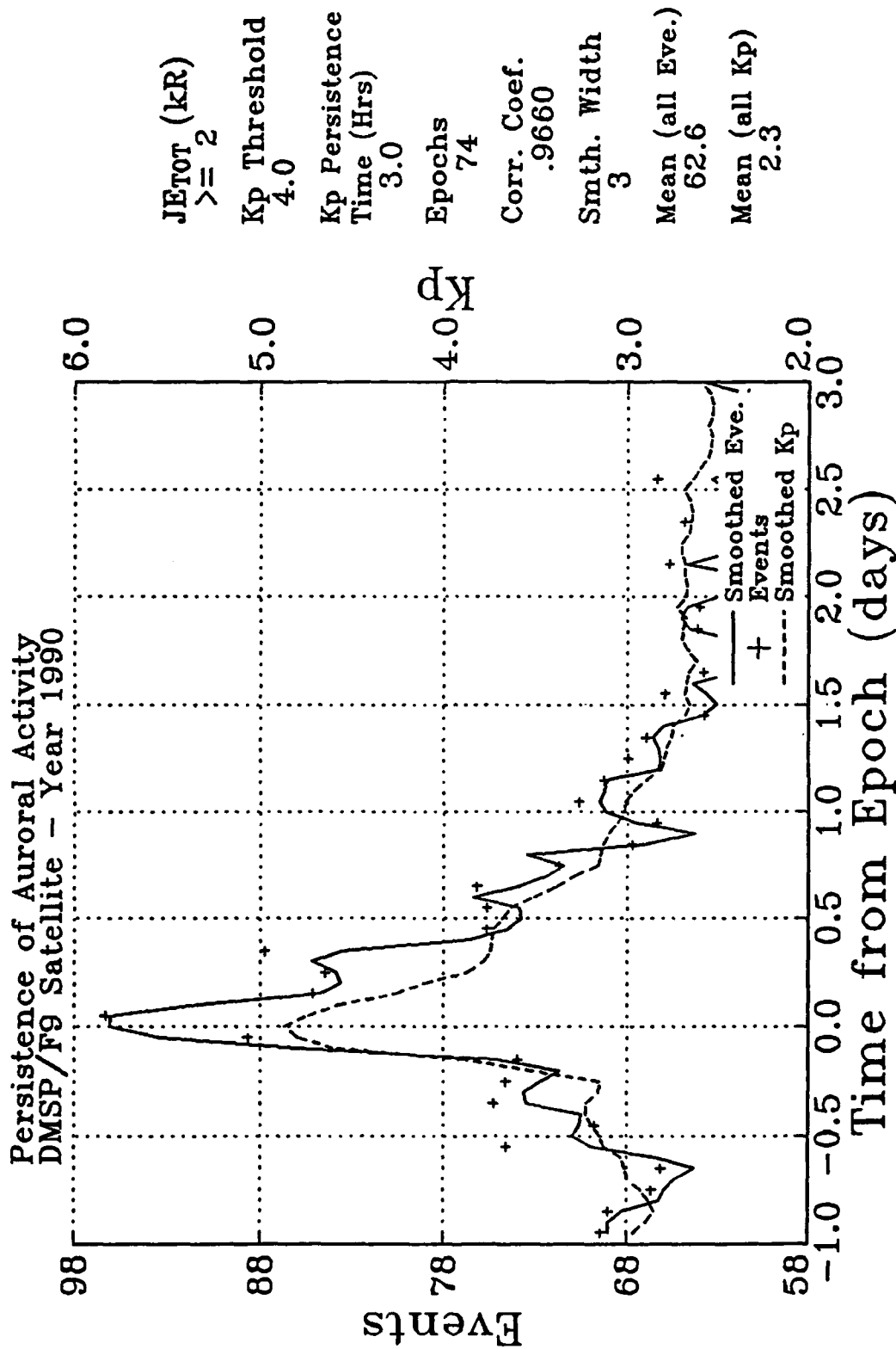


Figure 7(a). Comparison of Kp index with the number of events per hemispheric pass for energy fluxes (JE_{TOT}) greater than or equal to 2 kR over a time window of 4 days with a sampling rate of 1.2 hours. The solid line is the smoothed number of events which are the 3-point averages of the samples denoted by plus signs (+). The dashed line is the 3-point smoothed Kp. This figure is for a Kp threshold of 4.0 and a Kp persistence time of 3 hours.

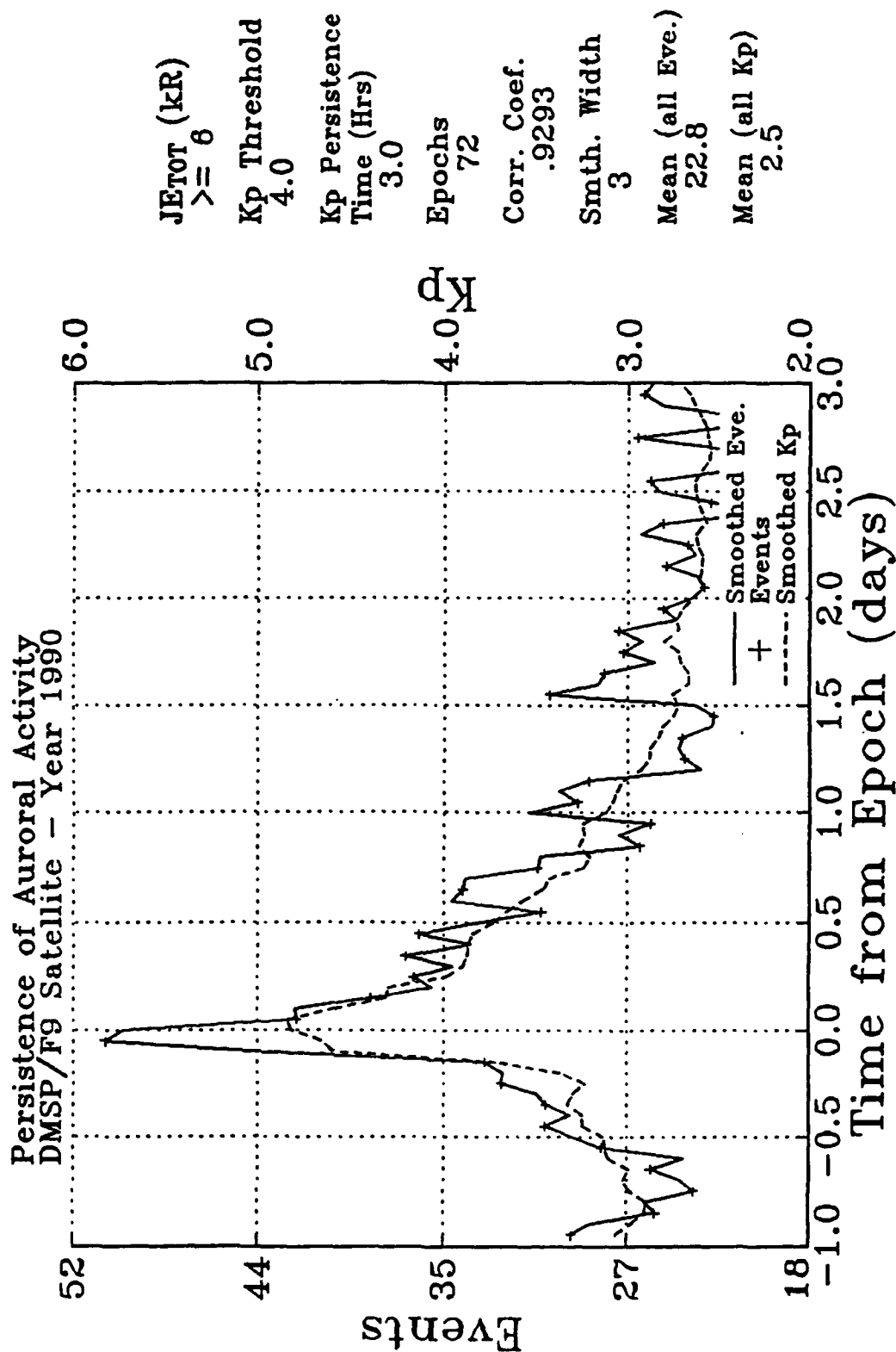


Figure 7(b). Same as Figure 7(a), but for an energy flux threshold of 6 kR.

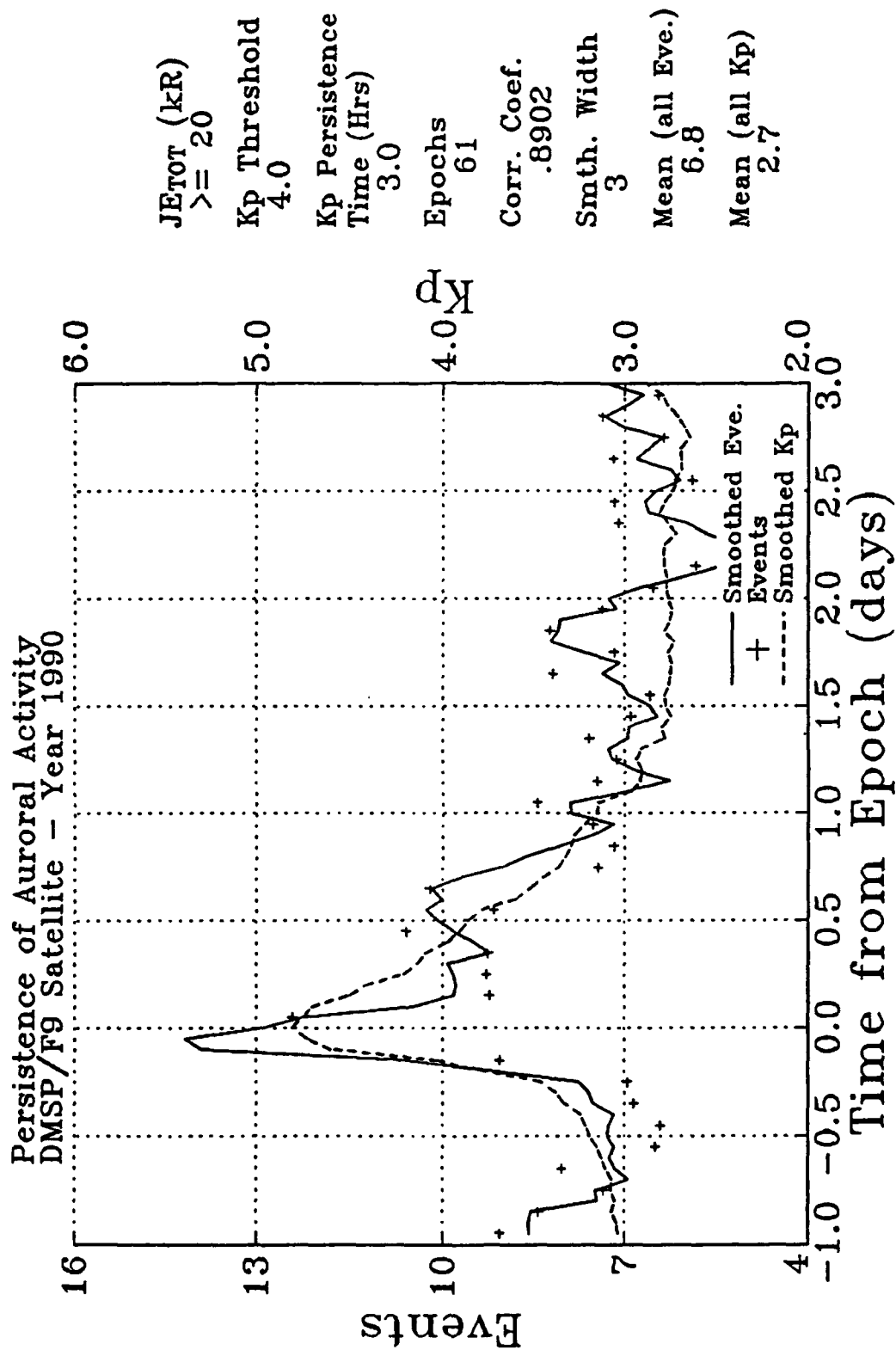


Figure 7(c). Same as Figure 7(a), but for an energy flux threshold of 20 kR.

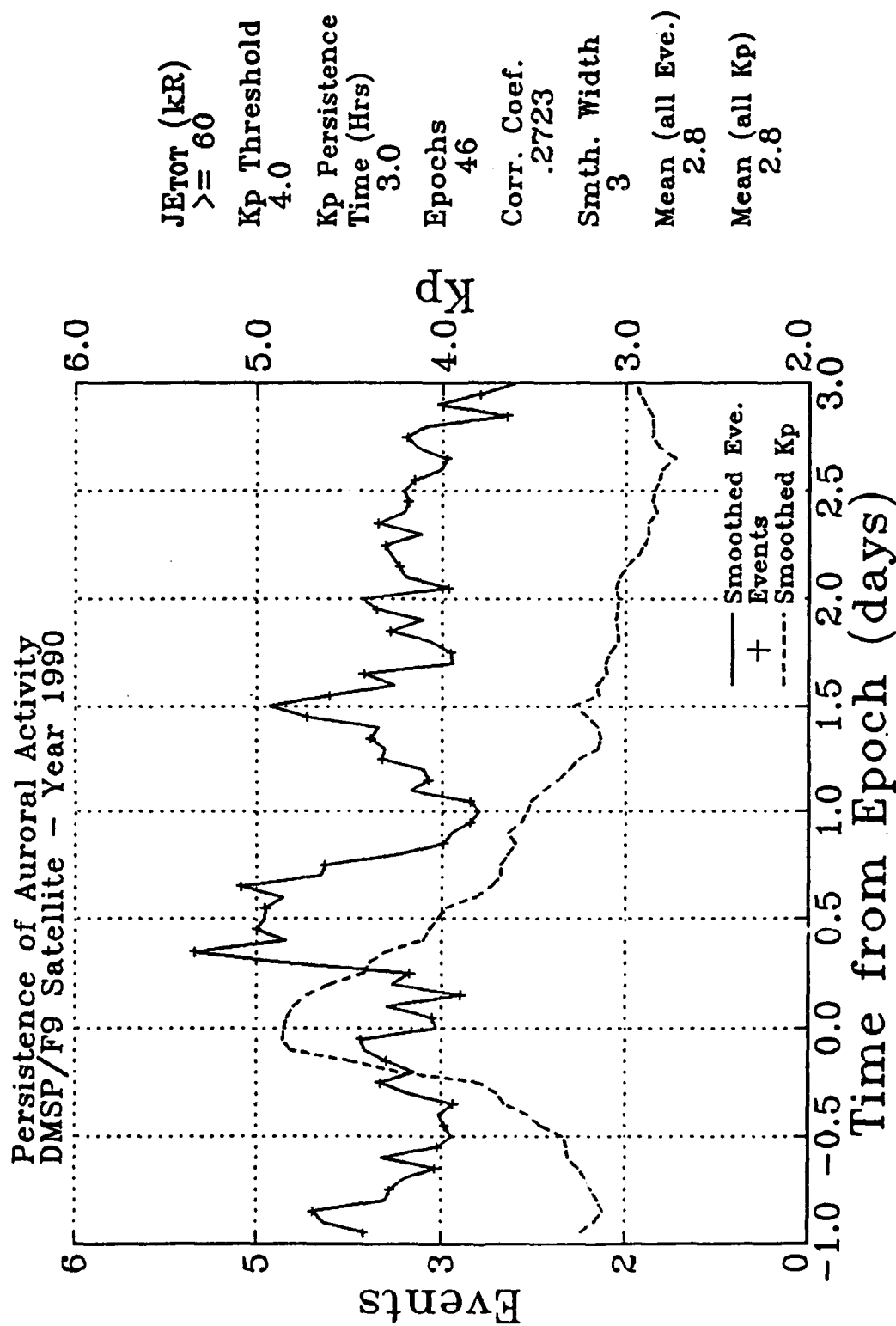


Figure 7(d). Same as Figure 7(a), but for an energy flux threshold of 60 kR.

ensemble average in estimating these quantities.

From the figures, the correlation coefficient is about 0.98 for events with JE_{tot} greater than or equal to 2 kR and 6 kR (Figures 7a and 7d), and drops to about 0.89 for $JE_{tot} \geq 20$ kR (Figure 7c). The results in Figure 7d are not reliable because of insufficient data samples. A correlation coefficient of 0.7 to 1.0 shows that the two time series are highly dependent. Hence, we can assert with certitude that the geomagnetic activity as represented by the Kp index and the auroral activity as measured by the precipitating electron events are highly correlated indeed.

5.0 CONCLUSION AND FUTURE STUDIES

The observation of enhanced Kp is generally indicative of increased number of bright arcs. The increase in the auroral activity of precipitating electrons is significant for only a limited time period. During this time, a high correlation between enhanced Kp and the number of bright arcs can be achieved. The waiting time to increase the chance of observing bright auroral arcs after enhanced Kp values are observed should be between 3 to 6 hours. Further, the substantial increase in the number of observations of intense events as a result of enhanced Kp lingers a maximum of 36 to 48 hours. After this time period, this number drops to the average number of random observations. In conclusion, the nearer the observation can be made to the time of elevated Kp, the better the chances for observing arcs.

This study also shows that increasing the persistence time of high Kp values above a certain threshold does not improve the likelihood of occurrence of intense auroral events. That is, the persistence or lingering of the enhanced geomagnetic activity (as seen in Kp values) does not mean that the probability of observing bright arcs is increased.

Future studies that can provide additional understanding of the auroral activity events can be readily accomplished using the existing data base. Two studies can be implemented using the present data base, which would certainly reveal important features in the electron auroral events that the present study did not cover.

One study would carry out a superposed epoch analysis on the number of electron events as a function of specified thresholds of the number of events and how long they persist above the threshold values. This differs from the present study in which the epochs are obtained based on the Kp threshold values and their persistence duration above these thresholds.

Another study would carry out a superposed epoch analysis on the probability of occurrence of electron events as a function of specified thresholds of the number of events and how long they persist above the threshold values. For each hemispheric pass, the occurrence of an event will be indicated by 1 and no occurrence by 0. This study would then yield an averaged probability distribution of occurrence of events around the zero epoch. A probability distribution of the auroral electron activity as a function of time can be a valuable tool in estimating the persistence of auroral events.

6.0 REFERENCES

Bounar, K. H., and D. A. Hardy, "Integral Probability of Occurrence of Auroral Electron Flux Events from DMSP/F9 Electron Measurements", PL-TR-92-2091

Jursa, A. S., Scientific Editor, Handbook of Geophysics and the Space Environment, Chapter 12, 1985, AFGL-TR-85-0315, ADA167000.

McNeil, W. J., and D. A. Hardy, Private Communication, 17 October 1985.

Nagai, "Space Weather Forecast: Prediction of Relativistic Electron Intensity at Synchronous Orbit", *Geophys. Res. Lett.*, 15, 425, 1988.

APPENDIX A. GEOMAGNETIC K_p INDEX AND AURORAL EVENTS

The geomagnetic K_p index and the number of auroral events with energy fluxes greater or equal to 2kR observed in each hemispheric pass. The data are based on the DMSP/F9 flux measurements in 1990. These curves are shown versus day number.

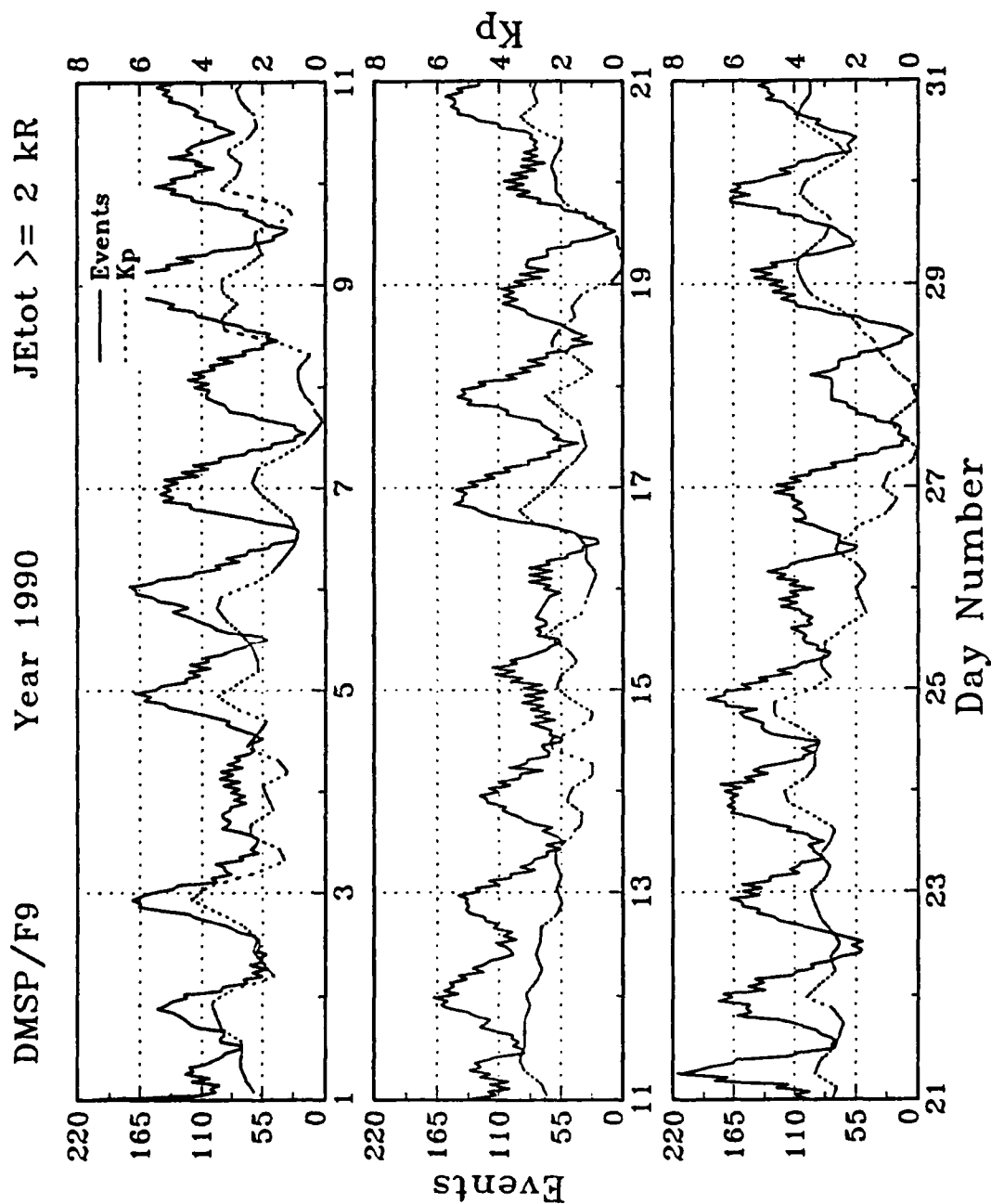


Figure A-1. Days 1 - 31.

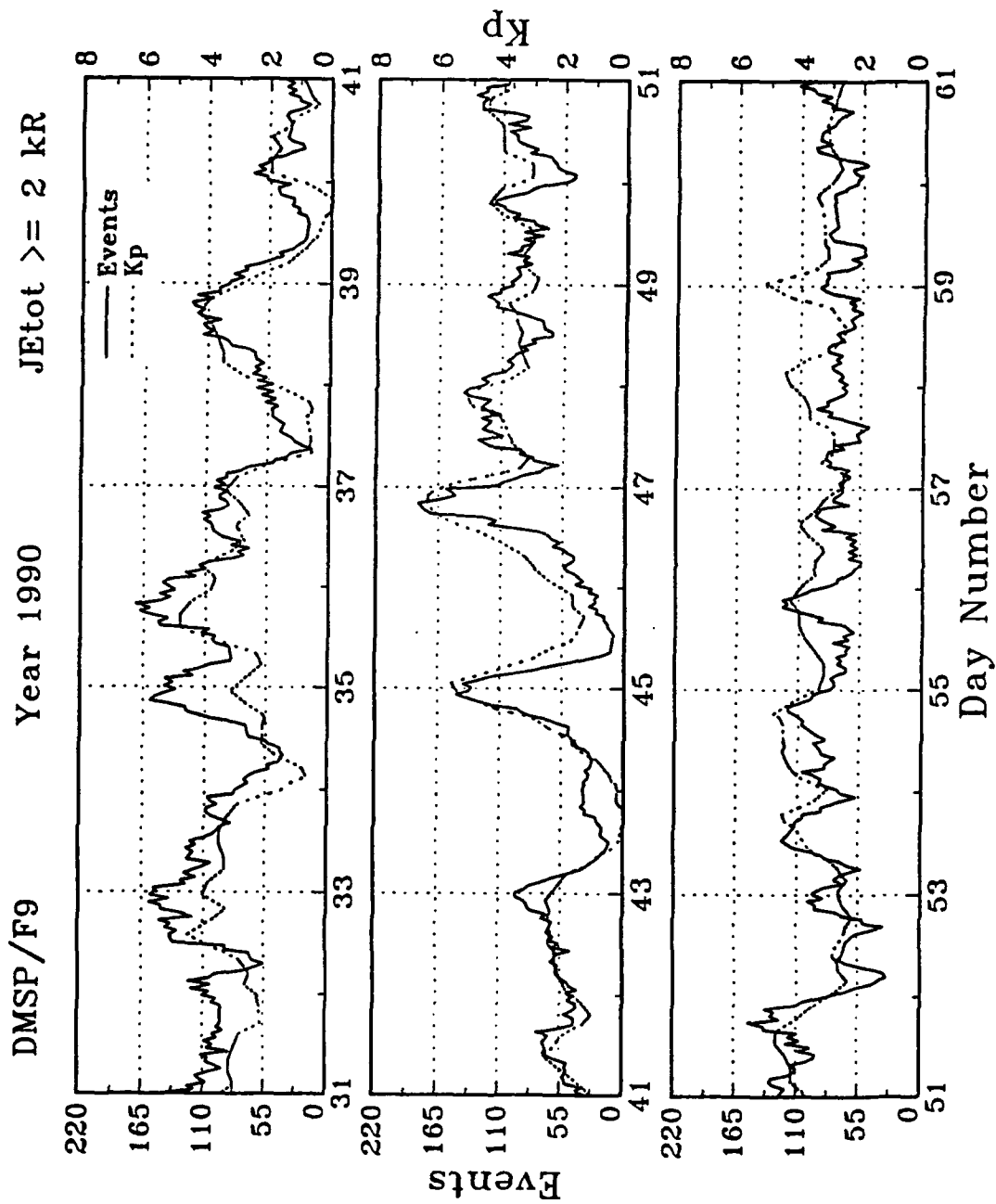


Figure A-2. Days 31 - 61.

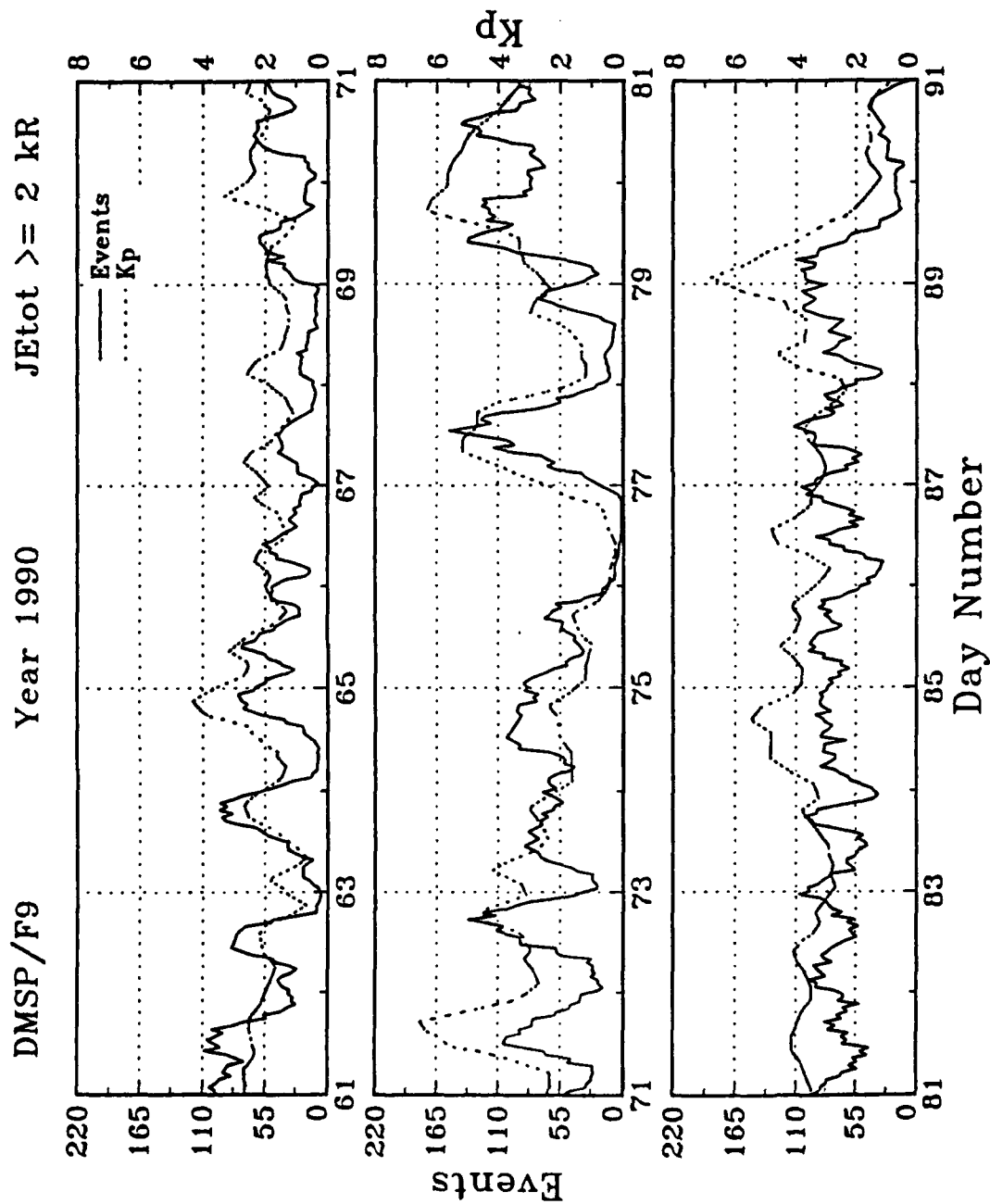


Figure A-3. Days 61 - 91.

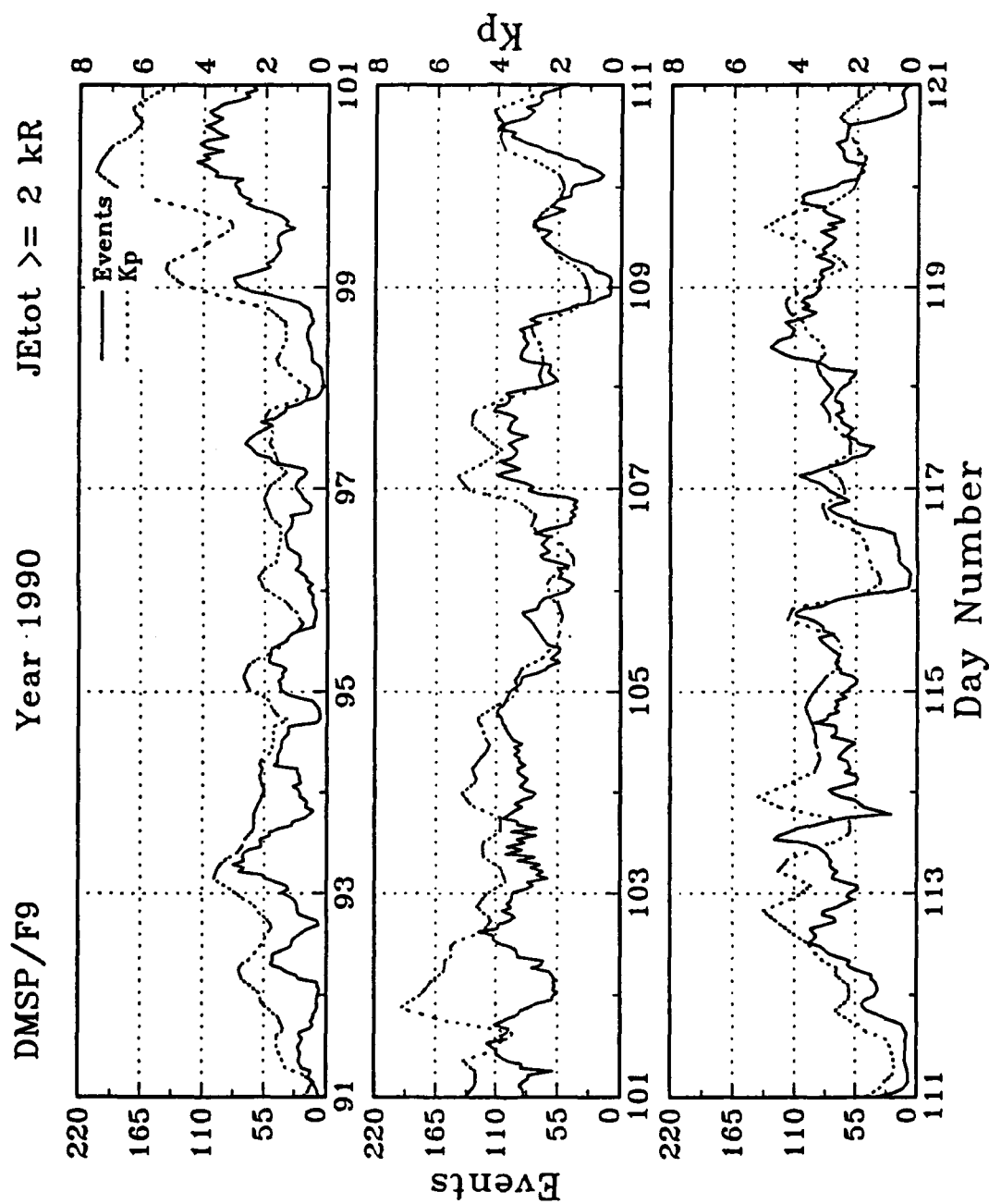


Figure A-4. Days 91 - 121.

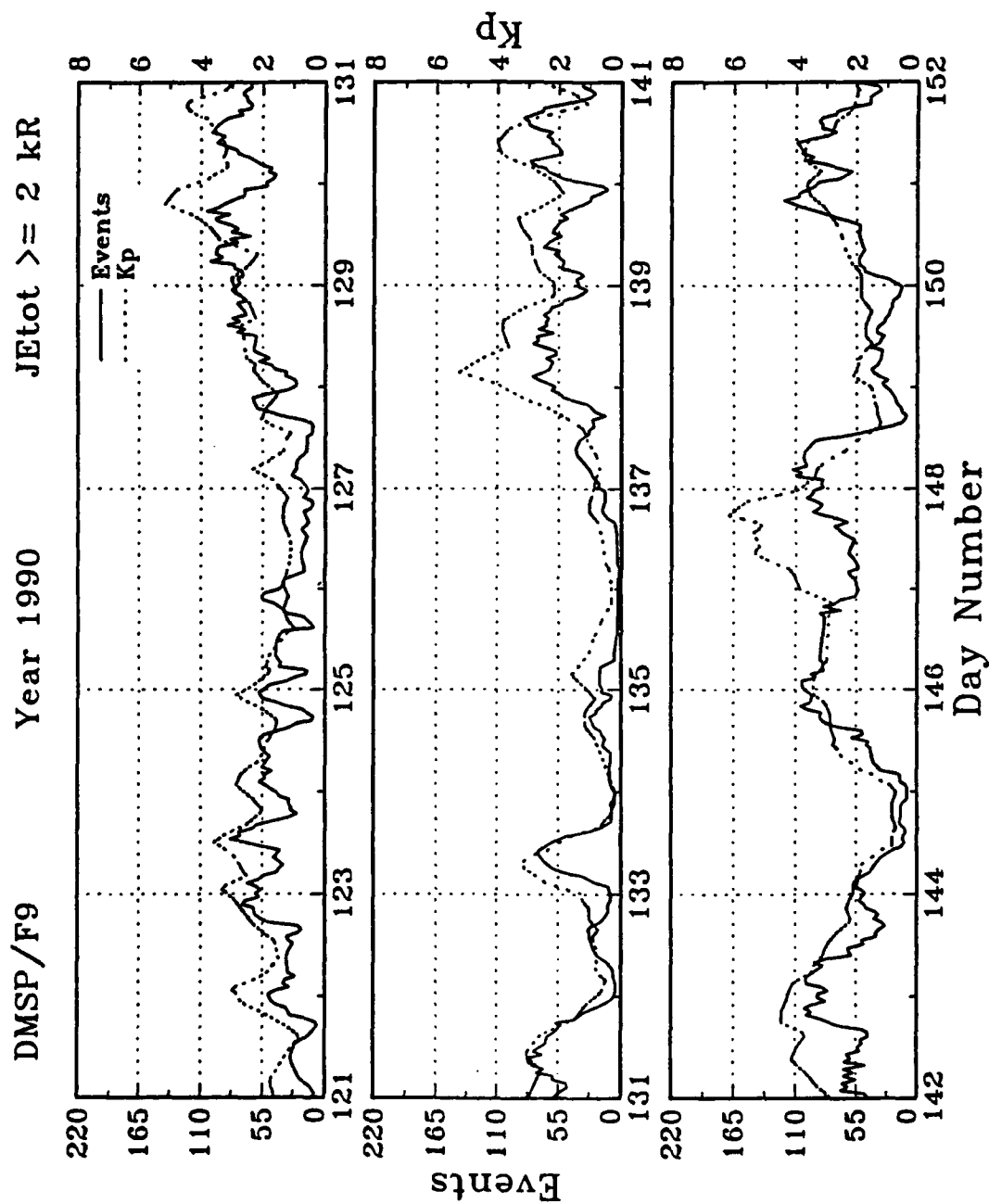


Figure A-5. Days 121 - 152.

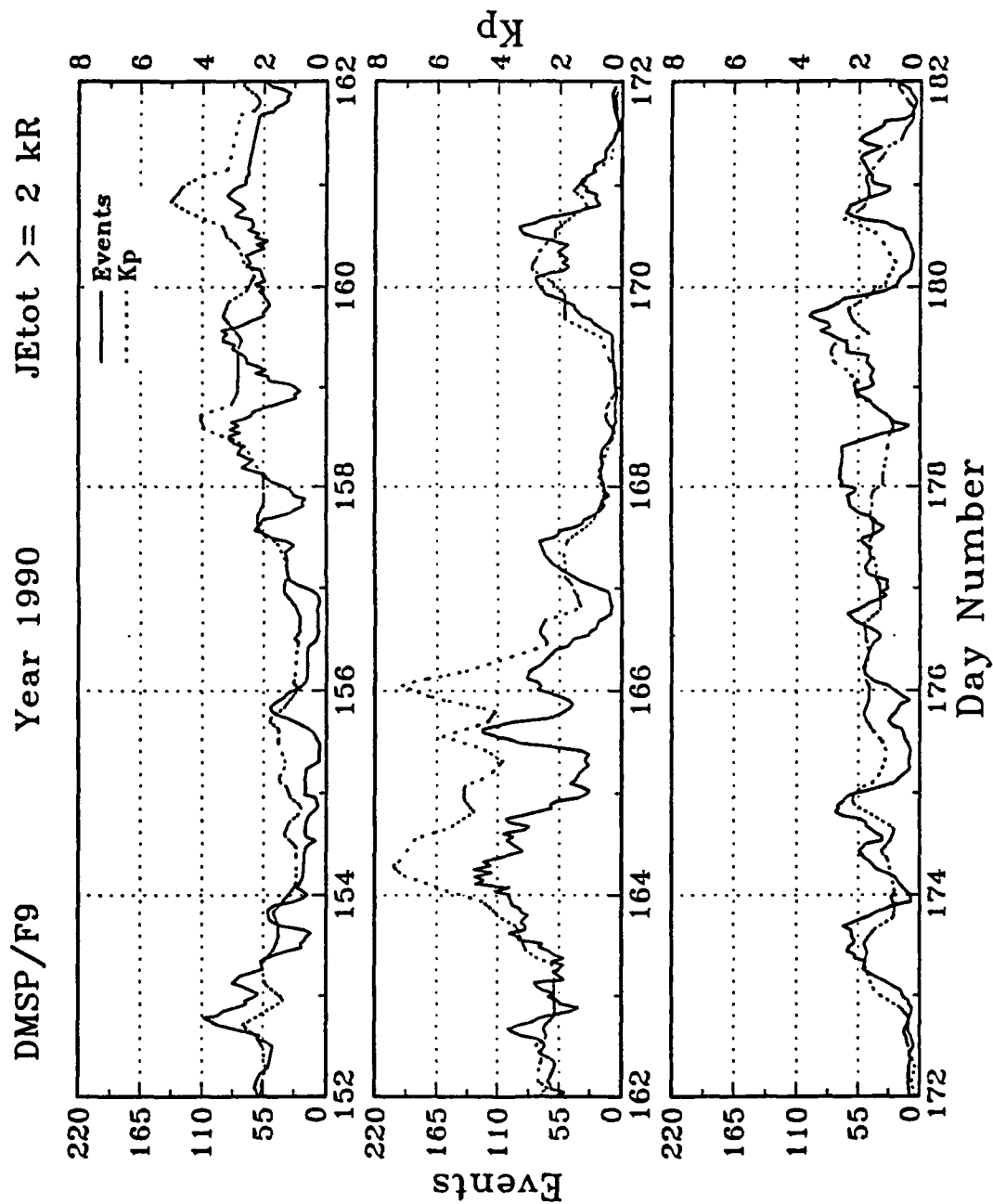


Figure A-6. Days 152 - 182.

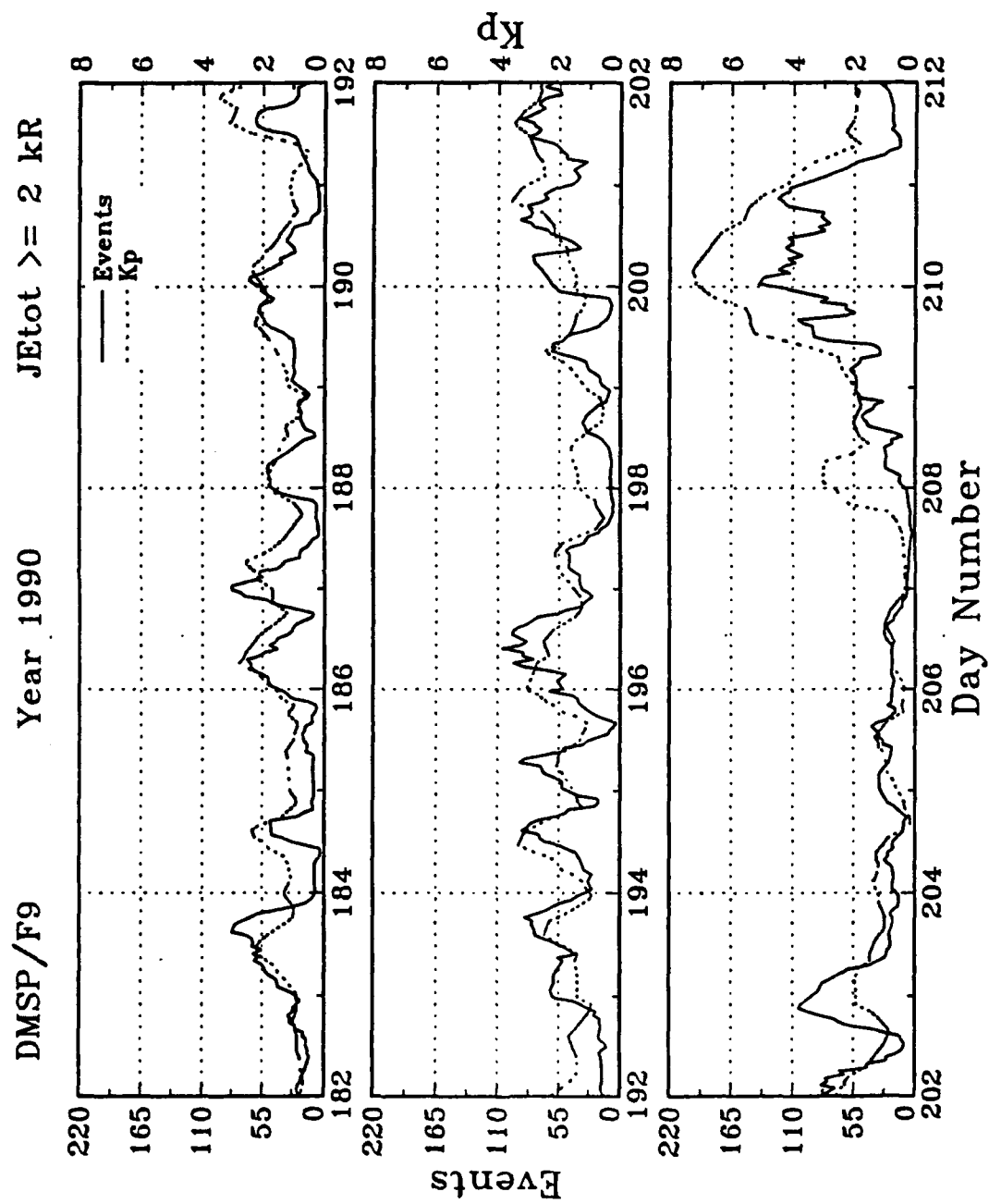


Figure A-7. Days 182 - 212.

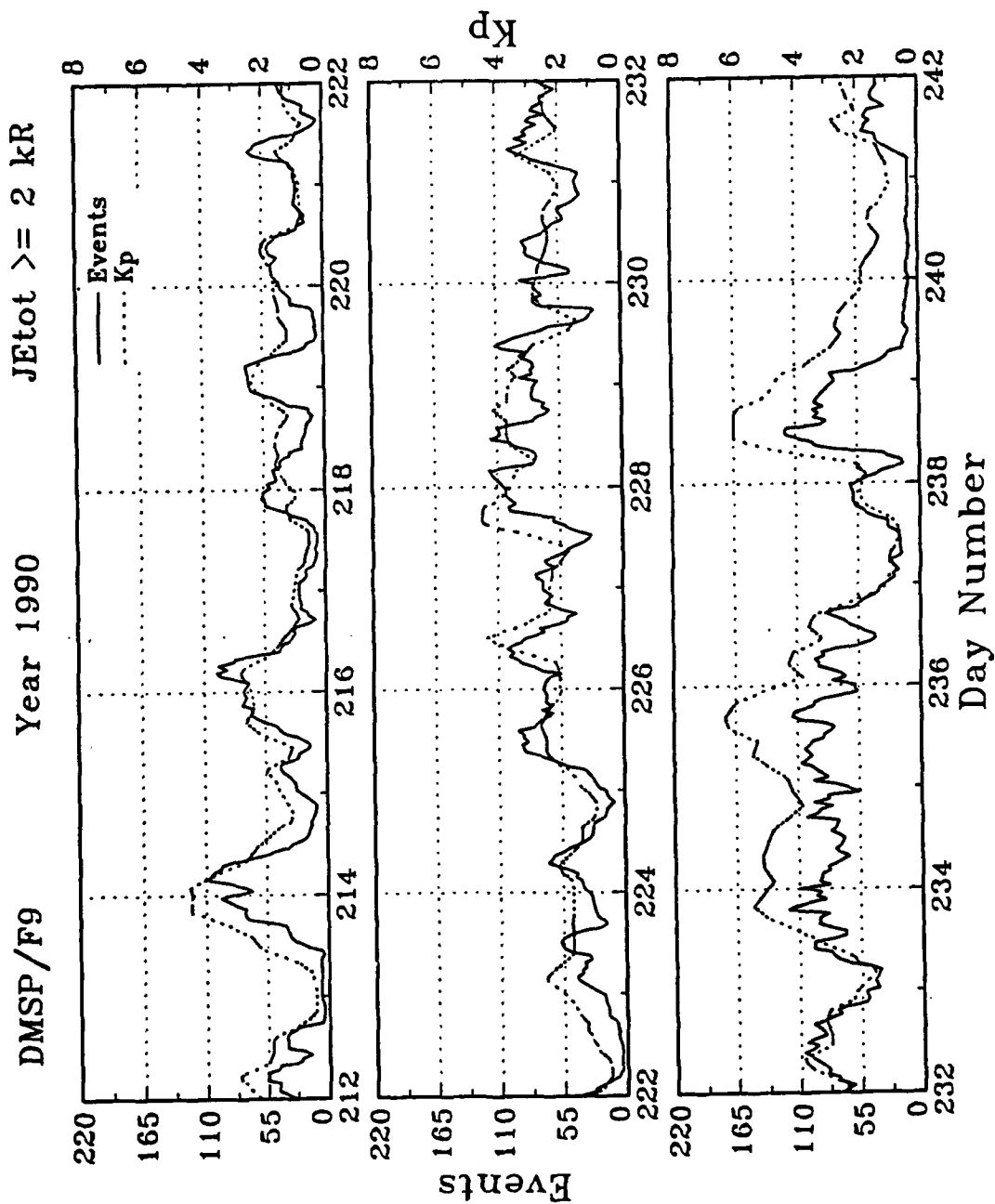


Figure A-8. Days 212 - 242.

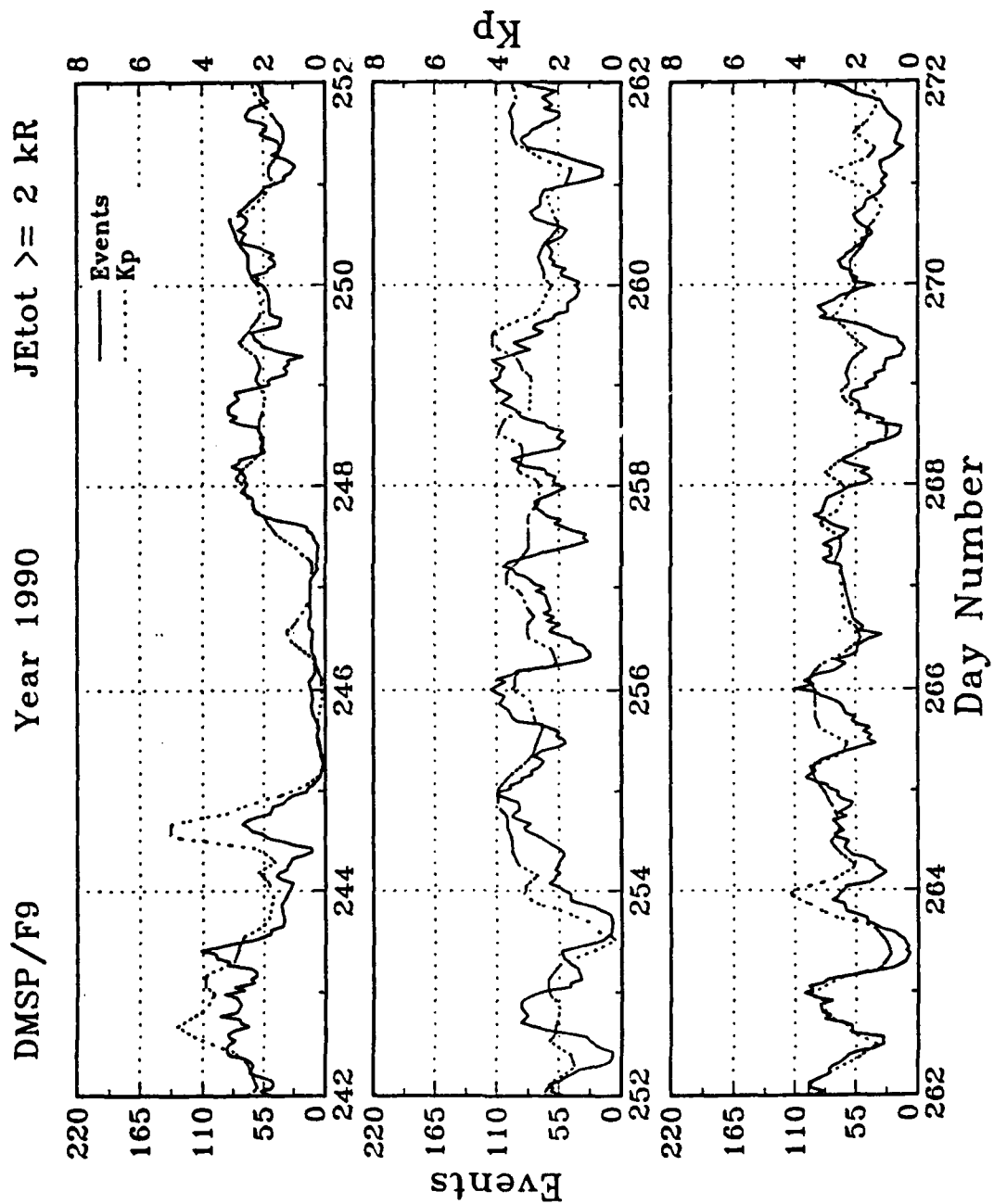


Figure A-9. Days 242 - 272.

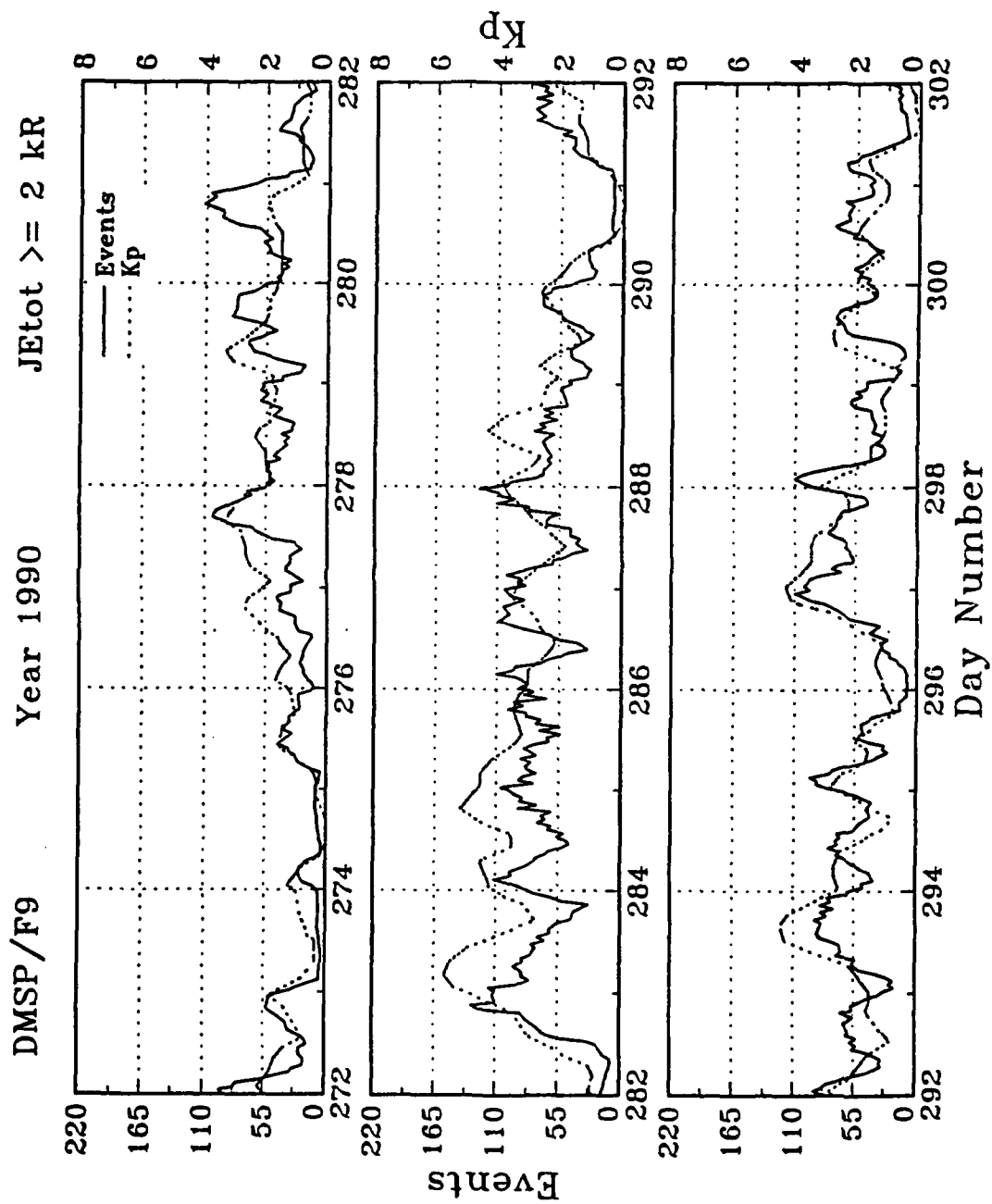


Figure A-10. Days 272 - 302.

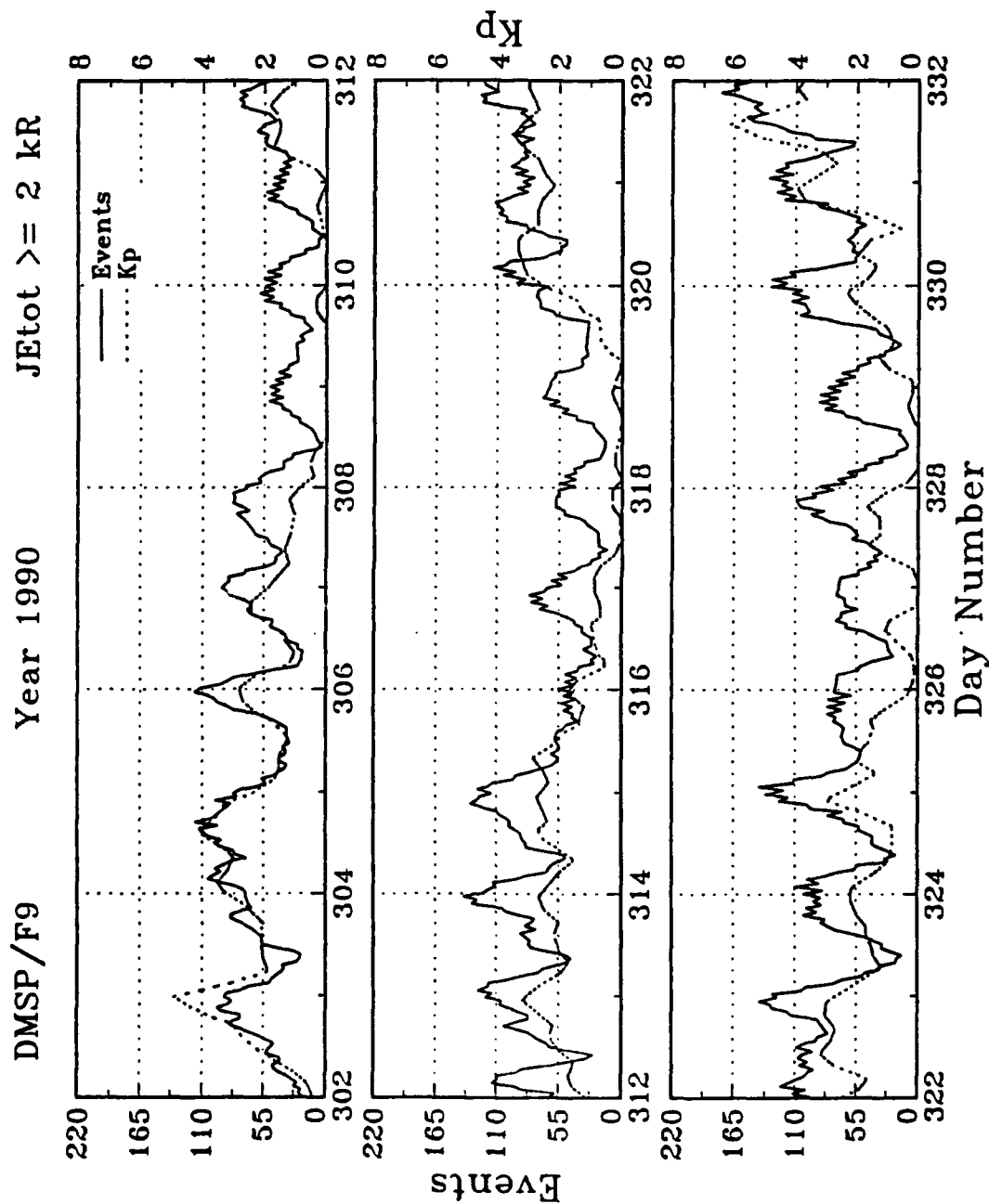


Figure A-11. Days 302 - 332.

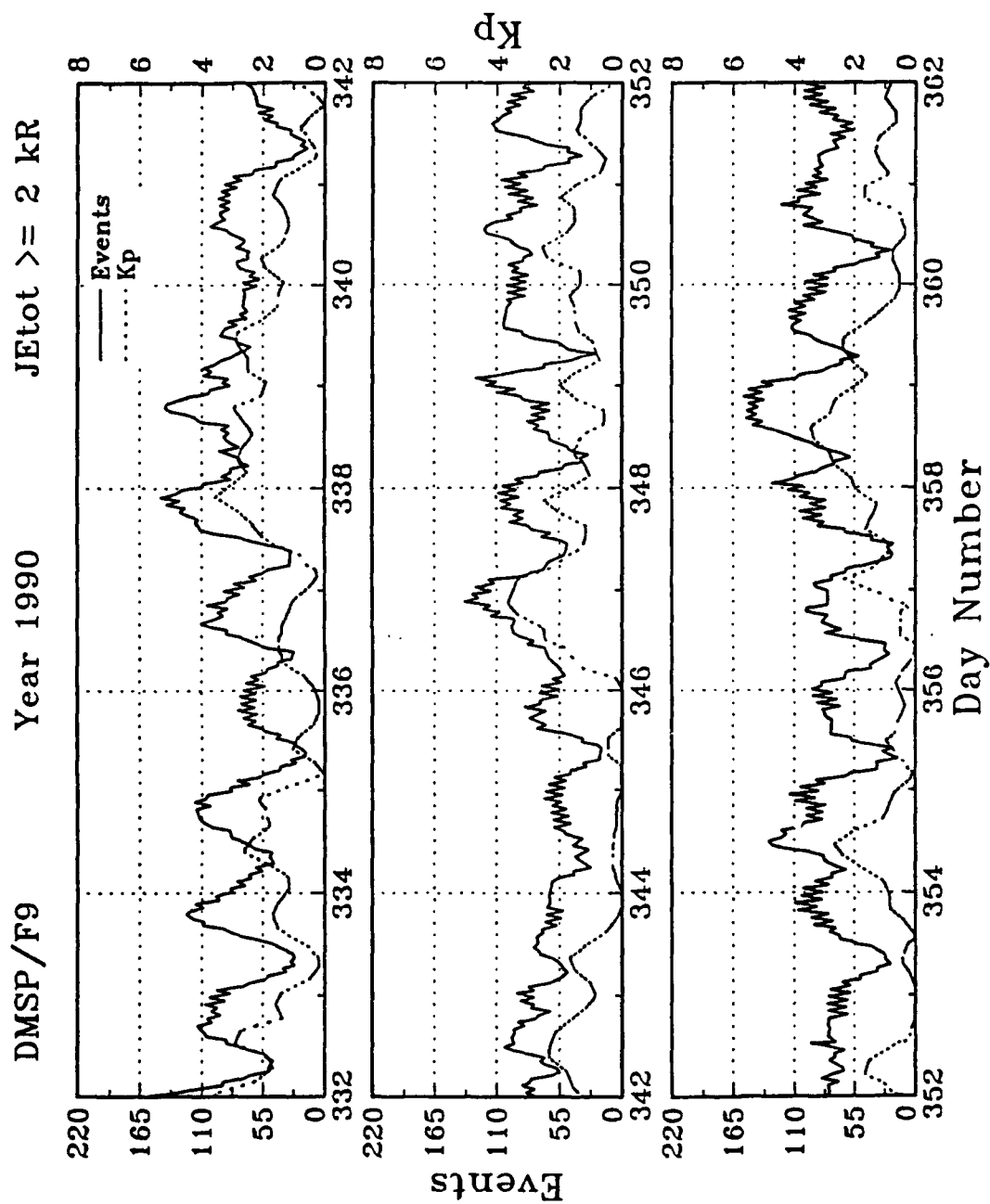


Figure A-12. Days 332 - 362.

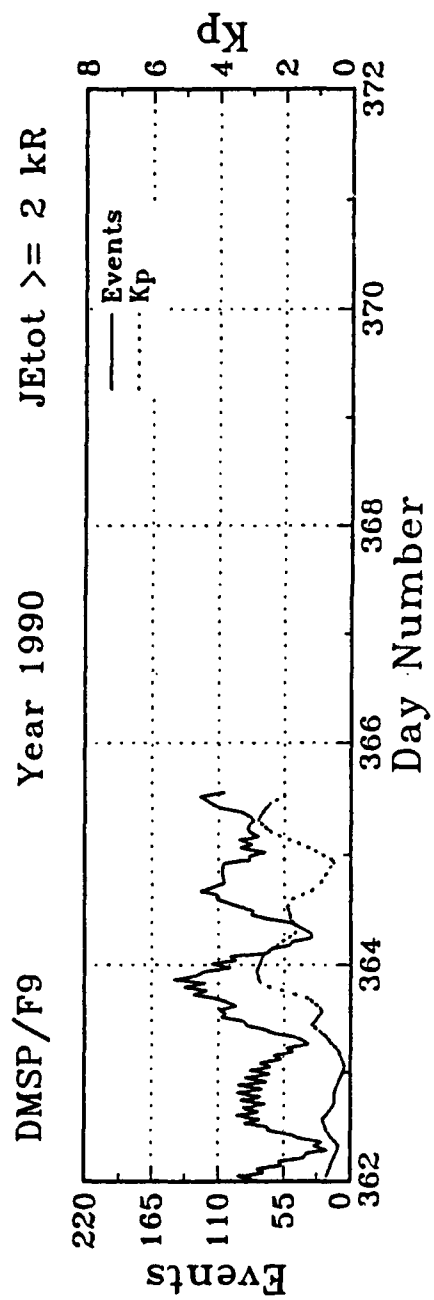


Figure A-13. Days 362 - 372.